PATTERNS IN NON-LINEAR GRAVITATIONAL CLUSTERING:

A NUMERICAL INVESTIGATION

T.Padmanabhan *, Renyue Cen, Jeremiah P. Ostriker, and F J Summers

Princeton University Observatory

Princeton, NJ 08544

email: cen@astro.princeton.edu

* Permanent address: IUCAA, Post Bag. 4, Ganeshkhind, Pune 411 007, India. email: paddy@iucaa.ernet.in

ABSTRACT

The nonlinear clustering of dark matter particles in an expanding universe is usually studied by N-body simulations. One can gain some insight into this complex problem if simple relations between physical quantities in the linear and nonlinear regimes can be extracted from the results of N-body simulations. Hamilton et al. (1991) and Nityananda and Padmanabhan (1994) have made an attempt in this direction by relating the mean relative pair velocities to the mean correlation function in a useful manner. We investigate this relation and other closely related issues in detail for the case of six different power spectra: power laws with spectral indexes $n = -2, -1$, cold dark matter (CDM), and hot dark matter models with density parameter $\Omega = 1$; CDM including a cosmological constant (Λ) with $\Omega_{CDM} = 0.4$, $\Omega_\Lambda = 0.6$; and $n = -1$ model with $\Omega = 0.1$. We find that: (i) Power law spectra lead to self-similar evolution in an $\Omega = 1$ universe. (ii) Stable clustering does not hold in an $\Omega = 1$ universe to the extent our simulations can ascertain. (iii) Stable clustering is a better approximation in the case of $\Omega < 1$ universe in which structure formation freezes out at some low redshift. (iv) The relation between dimensionless pair velocity and the mean correlation function, $\bar{\xi}$, is only approximately independent of the shape of the power spectrum. At the nonlinear end, the asymptotic value of the dimensionless pair velocity decreases with increasing small scale power, because the stable clustering assumption is not universally true. (v) The relation between the evolved $\bar{\xi}$ and the linear regime $\bar{\xi}$ is also not universal but shows a weak spectrum dependence. We

2

present simple theoretical arguments for these conclusions.

Cosmology: large-scale structure of Universe – cosmology: theory – galaxies: clustering –
numerical methods

1. INTRODUCTION

Large-scale structures (like galaxies, clusters etc.) are believed to have evolved primarily through the action of gravitational force out of small initial density perturbations. When these density perturbations are small, it is possible to study their evolution using linear theory. But once the density contrast becomes comparable to unity, linear perturbation theory breaks down and one must invoke either analytic approximations or direct N-body simulations to study the growth of perturbations.

Several people have performed extensive numerical simulations, with varying dynamic range and resolution, to study this problem. While these simulations are of value in making concrete predictions for specific models, they do not seem to have provided deep insight into physics of non-linear gravitational dynamics. To obtain such an insight into this complex problem, it is important to ask whether simple patterns in gravitational clustering can be extracted from the plethora of simulations. If such patterns are found, they will work as pointers for possible analytic approximations and could even eliminate the need for extensive simulations in some specific cases. We shall study, in this paper, the possible existence of such simple patterns in the nonlinear gravitational clustering.

It would be naive to hope for a simple picture to emerge in the full theory of structure formation, involving both gravitational and hydrodynamic processes. Radiative coupling of baryons and photons is a multiscale process with several dimensionless ratios, and it is unlikely that such processes can be described by simple universal rules. On scales less

than a few Mpc such physical effects become increasingly important. The situation is quite different as regards the dark matter in the universe, often assumed to be composed of collisionless, weakly interacting, massive particles. By limiting our consideration to the gravitational interaction alone, one may hope to uncover some basic relationships.

Section 2 discusses some possible scaling relations and motivates the numerical simulations we have done. Section 3 describes the simulations and last section presents the results and discussions.

2. PATTERNS IN NONLINEAR CLUSTERING

For the case of interest, we can describe the dark matter as a system of particles interacting via Newtonian gravity, at scales which are small compared to the Hubble radius. The motion of particles in this case can be described by the equations

$$\ddot{\mathbf{x}}_i + \frac{2\dot{a}}{a}\dot{\mathbf{x}}_i = -\frac{1}{a^2}\nabla\phi; \quad \nabla^2\phi = 4\pi G\rho_b a^2 \delta, \tag{1}$$

where $\mathbf{x}_i(t)$ is the comoving position of the i-th particle, $a(t)$ is the expansion factor, $\rho_b(t)$ is the background density in a matter dominated universe and ϕ is the gravitational potential due to the perturbed density $\delta\rho \equiv \rho - \rho_b \equiv \rho_b\delta$. All spatial derivatives are with respect to the comoving coordinates. In the fluid limit, the same system is described by the equations

$$\dot{\delta} + \nabla \cdot [(1+\delta)\mathbf{u}] = 0; \quad \dot{\mathbf{u}} + (\mathbf{u} \cdot \nabla)\mathbf{u} + \frac{2\dot{a}}{a}\mathbf{u} = -\frac{1}{a^2}\nabla\phi, \tag{2}$$

5

where $\mathbf{u} \equiv (d\mathbf{x}/dt)$. For a universe with density parameter $\Omega = 1$, we can introduce the time coordinate $\tau \equiv \ln(t/T)$ where T is an arbitrary positive constant and a rescaled potential $\psi \equiv (4/9) H_0^{-2} (a\phi)$ with H_0 the Hubble constant. Then equation (1) reduces to

$$\frac{d^2 \mathbf{x}_i}{d\tau^2} + \frac{1}{3} \frac{d\mathbf{x}_i}{d\tau} = -\nabla\psi; \quad \nabla^2 \psi = \delta, \tag{3}$$

while (2) becomes

$$\frac{\partial \delta}{\partial \tau} + \nabla \cdot [(1+\delta)\mathbf{p}] = 0; \quad \frac{\partial \mathbf{p}}{\partial \tau} + (\mathbf{p} \cdot \nabla)\mathbf{p} + \frac{1}{3}\mathbf{p} = -\nabla\psi, \tag{4}$$

where $\mathbf{p}$ is the velocity field corresponding to τ coordinate. All reference to the background spacetime has completely disappeared in these equations. Hence these equations have no intrinsic scale. If we now further assume that the initial power spectrum of perturbations is scale invariant with $P(k) = Ak^n$, then we expect the dynamical evolution of such a system to possess some universal characteristics.

To avoid misunderstanding, we stress several points. First, any particular realization of an initial power spectrum will have scales appearing in it randomly. When averaged over an ensemble of realizations with the same $P(k)$, these scales will disappear. Second, the use of a grid to generate initial conditions will introduce a scale of order the mean interparticle distance. Such scales are erased by evolution, except in the most underdense void regions. Third, softening in the gravitational force introduces a minimum resolution scale which cannot be avoided. We shall, however, concentrate on scales which are larger than the softening scale to obtain reliable conclusions. Fourth, requirements of convergence,

6

$(n > -3)$, and the generation of a k^4 tail due to discreteness effects restrict the range of n to $-3 < n < 4$. If equations (2) are studied perturbatively, spurious divergences due to long wavelength modes can arise for $-3 < n < -1$. The long wavelength contribution to bulk velocity, for example, has a divergent contribution for $n = -2$ when handled perturbatively. The nonperturbative argument given in the paragraph above clearly shows that these divergences are spurious. Thus endpoint effects should not be important for $-3 < n < 4$ and thus no physical scales enter the problem for $\Omega = 1$.

One immediate consequence of the above analysis is that a simple scaling relation *must* exist in all simulations involving dark matter with power law spectrum, in an $\Omega = 1$ universe. Since there is no a priori scale in the problem, the natural length at any time is $x_{\mathrm{NL}}(a)$, the comoving scale which is going nonlinear at the epoch a. Thus all dimensionless physical parameters must be expressible as a universal function of (x/x_{NL}). For example, we expect the correlation function $\xi(x, a)$ to have the form $\xi(x, a) = f_n[x/x_{\mathrm{NL}}(a)]$. This implies that the evolution is self-similar, and ξ is completely specified by a single function f_n which depends on the index n.

Further progress can be achieved if we assume that clustering at the extreme nonlinear end is "stable" (Peebles 1980). In such a case, $\xi(a, x)$ must have the form $\xi(a, x) = a^3 F(ax)$ in the extreme nonlinear limit, because the number density of objects in collapsed regions is assumed constant, while the average density of the universe decreases as a^{-3}. This assumption is equivalent to the postulate that highly overdense, virialized objects maintain

7

their identities, i.e., merging and fragmentation either do not occur or occur at strictly balancing rates. The assumption of self-similarity requires that the correlation function at the linear end evolves as $\xi_L \propto a^2 x^{-(n+3)}$. Combining this result with the stable clustering postulate, it is easy to show that

$$\xi(a, x) \propto a^3 (ax)^{-\gamma} \propto a^{6/(n+5)} x^{-3(n+3)/(n+5)}, \tag{5}$$

in the extreme nonlinear end. In other words, the index of the nonlinear correlation function γ should be related to the index of the linear power spectrum n by

$$\gamma = \frac{3(n+3)}{(n+5)}, \tag{6}$$

if the stable clustering ansatz were true. Therefore, given the correlation function in the linear theory, ξ_L, it is possible to determine the correlation function in the nonlinear theory up to a constant factor provided we assume the validity of stable clustering. In section 4 we examine the quantitative accuracy of the above two assumptions.

Equation (6), however, is not very useful in practice. To begin with, it works only in the *extreme* nonlinear regime and one is often interested in the intermediate scales. Second, it does not provide any clue to the amplitude of the nonlinear correlation function in terms of the linear one. Third, it is based on the assumption that the power spectrum is strictly scale free. And finally, it rests on the ad hoc assumption of stable clustering.

Attempts have been made to generalize this idea by using an effective index n_{eff} as a function of scale, defined as,

$$n_{\text{eff}} \equiv \frac{d \ln P}{d \ln k}. \tag{7}$$

8

Nityananda & Padmanabhan (1994, hereafter NP) found that a simple implementation of scaling using n_{eff} does not work satisfactorily in that a smooth transition between linear and non-linear regimes is not obtained. It is important, therefore, to look for more sophisticated - yet manageable - rules which will provide information about the nonlinear theory in terms of the linear theory.

One such attempt was made in NP along the following lines: They assumed that the mean relative pair velocity of particles $v_p(a, x)$ can be expressed in the form

$$v_p(a, x) = -\dot{a}xh[\bar{\xi}(a, x)], \tag{8}$$

where $\bar{\xi}$ is the average correlation function within a sphere of radius x and h is a universal function of its argument. Given this ansatz, NP show that it is possible to relate the mean correlation function $\bar{\xi}$ to the mean linear correlation function $\bar{\xi}_L$ by the relation

$$\bar{\xi}_L(a, l) = \exp\left(\frac{2}{3}\int^{\bar{\xi}(a,x)} \frac{d\nu}{h(\nu)(1+\nu)}\right), \tag{9}$$

with $l \equiv x[1 + \bar{\xi}(a, x)]^{1/3}$. Earlier work by Hamilton et al. (1991) suggested that such a relationship seems to be borne out by the numerical simulations. In other words, numerical simulations seem to suggest that the function $h(\bar{\xi})$ is universal; it is independent of the epoch *and* the power spectrum used in the simulations. This function seems to behave as follows: $h(\bar{\xi}) \approx (2/3)\bar{\xi}$ for $\bar{\xi} \ll 1$, reaches a maximum of about 2 at $\bar{\xi} \approx 20$ and decreases to about unity at large $\bar{\xi}$. For a wide class of power law spectra and spectra similar to that of cold dark matter (CDM), the relationship in (5) can also be expressed as

9

$$\bar{\xi}(a, x) = \begin{cases} \bar{\xi}_L(a, l) & \text{(for } \bar{\xi}_L < 1.2, \bar{\xi} < 1.2) \\ 0.7[\bar{\xi}_L(a, l)]^3 & \text{(for } 1.2 < \bar{\xi}_L < 6.5, 1.2 < \bar{\xi} < 195) \\ 11.7[\bar{\xi}_L(a, l)]^{3/2} & \text{(for } 6.5 < \bar{\xi}_L, 195 < \bar{\xi}) \end{cases} \tag{10}$$

This fitting function is due to Bagla and Padmanabhan (1993) and captures the essence of a more complicated fit given in Hamilton et al (1991).

Unlike the self-similarity argument mentioned earlier, this relation cannot be independent of the power spectrum in the strict sense. To see this, consider a power spectrum with a sharp maximum at $x \approx L$ and very little small scale power. [This is similar to the HDM spectrum]. The first scales which go nonlinear will correspond to clusters with size $x \approx L$. The evolution of the first nonlinear structures in such a model could be well approximated by collapse of a spherical top hat (STH), since there is very little small scale power. For an STH model, one can easily show that h is a monotonically increasing function of the density contrast $\delta \approx \bar{\xi}$ and $h \approx \bar{\xi}^{1/2}$ as $\bar{\xi} \to \infty$ (see the discussion in section 4 below). This suggests that h will increase with $\bar{\xi}$ for a good range of $\bar{\xi}$ in the HDM-like models until significant amount of small scale power develops. One can reach the same conclusion from (10) as well: If there is very little small scale power in linear theory, then $\bar{\xi}$ will have to rise far more steeply with $\bar{\xi}_L$ (in the nonlinear end) than suggested by (10).

The study of such an extreme example suggests that there might exist a weak spectrum dependence in the $h(\bar{\xi})$ relation even in more moderate cases. Broadly speaking, we expect h to be lower at a given $\bar{\xi}$ (in the nonlinear regime with $\bar{\xi} > 10$ or so) as we add more small

scale power. If stable clustering is invoked, then it is possible to motivate this conclusion along the following lines:

Consider a spherical region of initial radius r_i and overdensity $\nu\sigma$ where $\sigma = \sigma_0 r_i^{-(n+3)/2}$ is the variance of the gaussian density fluid. In a spherical model, this region will expand to a maximum radius of about $(r_i/\nu\sigma)$ and virialise to a final radius $r \equiv \lambda(r_i/\nu\sigma) = (\lambda/\nu\sigma_0) r_i^{\frac{n+5}{2}}$ where $\lambda \approx 0.5$. We shall assume that the coorelation function at the nonlinear end $\xi_{NL}(r)$ is contributed by such virialised objects and can be computed as

$$1 + \xi(r) \approx \xi(r) = \langle \left(\frac{r_i}{r}\right)^3 \rangle. \tag{11}$$

This assumption is equivalent to the stable clustering hypothesis. From $r = (\lambda/\nu\sigma_0) r_i^{(n+5)/2}$, it follows that

$$\xi(r) = \left(\frac{\sigma_0}{\lambda}\right)^{6/(n+5)} r^{-\frac{3(n+3)}{(n+5)}} \left\langle \nu^{6/(n+5)} \right\rangle. \tag{12}$$

Assuming that ν is a gaussian variable, we get

$$\langle \nu^{6/(n+5)} \rangle = \frac{1}{\sqrt{2\pi}} 2^{\frac{1-n}{2n+10}} \Gamma\left(\frac{n+11}{2n+10}\right). \tag{13}$$

Equations (12) and (13) show that $\xi(r) \propto \xi_L^{3/2}[l]$ with $l \approx r\xi^{1/3}$; however, the proportionality constant has a weak n-dependence.

The averaging in (11) can be made more sophisticated by using a weightage proportional to r_i^m. In that case, we still obtain the same r dependence but the gamma function becomes

$$c = \sqrt{\pi} \frac{\Gamma\left(\frac{n+11+2m}{2n+10}\right)}{\Gamma\left(\frac{n+5+2m}{2n+10}\right)}. \tag{14}$$

This reduces to the above result when $m = 0$; recently, Mo et al. (1995) have suggested a model based on $m = 3$, which – of course – leads to similar conclusions.

While the above arguments suggest that $h[\bar{\xi}]$ will have a weak spectrum dependence, they depend crucially on the assumption of stable clustering. The $\xi(r)$ can be modelled by virialised clusters only if stable clustering is valid. This statement is independent of the actual averaging process used in (12). Because of this reason, arguments like the above ones – and the n dependence obtained from them – are unreliable. *If the system does not obey stable clustering criterion, $h[\xi]$ may still show an n-dependence but it cannot be obtained from the above argument.* On the other hand, a theoretical explanation for the approximate universality (and the deviations from it) will go a long way in providing an analytic description of the nonlinear evolution of gravitating particles. It is, therefore, important to test this ansatz as precisely as possible in as diverse cases as possible. In particular, one must ask: (i) Do the relations $h = h\left(\bar{\xi}\right)$ and equations (10) have a weak spectrum dependence for pure power law spectra in $\Omega = 1$ universe? (ii) How are the relations modified if the spectrum is not a pure power law? and (iii) What happens when

12

the background universe is not described by a matter dominated, $\Omega = 1$ model? We present the results of such a numerical investigation in this paper.

3. NUMERICAL MODELING

Two kinds of N-body simulations are used to simulate the evolution of the particles. The first one uses a standard Particles-Mesh code (PM, *cf.* Hockney & Eastwood 1981; Efstathiou *et al.* 1985) with the staggered mesh scheme (see, e.g., Park 1990; Cen 1992). We use $240^3 = 10^{7.1}$ particles on a 720^3 mesh with a simulation box size of $128h^{-1}$Mpc giving a spatial resolution of $0.18h^{-1}$Mpc and mass resolution of $4.2 \times 10^{10}\Omega h^{-1}M_\odot$. Gravitational force is calculated using an FFT technique coupled with the cloud-in-cell scheme to calculate the density as well as to assign the gravitational force to the positions of particles.

The second kind of simulations uses the P3MG3A code (Brieu, Summers, & Ostriker 1995). This code is based on the Particle-Particle-Particle-Mesh (P^3M) scheme (Efstathiou and Eastwood 1981; Efstathiou *et al.* 1985) utilizing a special gravity processor called GRAPE 3A (Okumura *et al.* 1993) to compute the PP part. Each simulation uses $128^3 = 10^{6.3}$ particles on a 256^3 mesh with a simulation box size of $128h^{-1}$Mpc. The Plummer softening length is set to be 1/20 of the mesh cell size, giving a nominal spatial resolution of $0.025h^{-1}$Mpc and a mass resolution of $2.8 \times 10^{11}\Omega h^{-1}M_\odot$.

Six different models are considered and are listed in Table 1. In the table, L_{box} refers to the one dimensional size of the computational cube, l_{res} lists the nominal resolution scale,

13

and σ_8 gives the linear value of the rms fluctuations in the mass on a sphere of radius $8\ h^{-1}$ Mpc at redshift zero. We adopt the transfer functions of Bardeen *et al.* (1986) for the standard CDM and HDM models. The power spectrum of the CDM+Λ model is from Cen, Gnedin, & Ostriker (1993). The initial density fields for each simulation are generated assuming Gaussian fluctuations and the initial velocity field is obtained using the Zel'dovich approximation.

4. RESULTS AND DISCUSSION

The above simulations were utilized to both examine the assumptions and explore the consequences of the arguments in §2. The important points to address are the self-similarity of scale free simulations, the validity of stable clustering, the universal nature of the relation between the dimensionless pair velocity and the mean correlation function, and the dependencies on spectral index. We discuss each of these features below:

We begin by verifying the self-similar nature of the evolution for power law spectra by testing whether $\xi(a, z)$ can be expressed as $\xi[x/x_{nl}(a)]$. This question was investigated earlier by Efstathiou et al. (1988) who obtained results which were somewhat different from ours. We have now repeated this analysis with better resolution and range for $n = -2, -1$ and we find that *self-similarity is borne out* in our simulations as expected. For the case $n = -1$ the fit is excellent. For $n = -2$ it is less good but, we believe, adequate. Figures (1a,b) show the two-point correlation function as function of x/x_{nl} (where x_{nl} is the scale corresponding to $\xi = 1$ at three different redshifts $z = 0.0, 0.5, 1.0$ for $n = -2, -1$ models. Note that the curves fall on top of each other. Also shown (as two dashed lines in each figure) are asymptotic slopes at the extreme nonlinear and linear ends. This result is expected based on the theoretical arguments given in section 2, but serves as a good check on the accuracy of simulations. In addition, it clarifies certain doubts raised in Efstathiou et al. (1988) regarding self-similarity for the case $n = -2$. On all the figures we only plot the points which correspond to scales (separations) larger than 2.5 cells in the PM simulations and twice the softening lengths in the P^{3}M simulations, which represent the true resolutions of two types of simulations.

It may be noted that in the case of $n = -1$, the linear slope extends to the quasi-linear regime as well, up to about $\bar{\xi} \approx 10$. This fact can be understood from equation (10). In

15

the quasi-linear regime, this equation predicts the evolution

$$\bar{\xi} \propto a^{\frac{6}{(n+4)}} x^{-\frac{3(n+3)}{(n+4)}},$$ (15)

so that $\bar{\xi} \propto a^2 x^{-2}$ for $n = -1$ in the quasi-linear regime as well. In other words, the linear and quasi-linear evolution has the same a and x dependence for $n = -1$. (See Bagla and Padmanabhan, 1995 for a more detailed discussion of this point.)

For comparison, We also show in Figures (1c,d,e,f) the corresponding results for the other four models (listed in Table 1): SCDM (1c), HDM (1d), LCDM (1e), and open $P_k = k^{-1}$ (1f) models, respectively. All these models have a characteristic scale and the low-Ω models have that feature even at the highest redshift probed. This should lead to deviations from self-similarity in figures 1 c - e. Such a deviation is apparent in the case of HDM (which has the strongest scale dependence), somewhat less apparent but noticeable in the case of CDM + λ and CDM (in which the scale dependence is weaker) and ambiguous in the case of open $n = -1$. This is essentially due to the fact mentioned above: $n = -1$ is special in the sense that linear evolution holds even for the quasi-linear regime. Hence the deviations are somewhat offset in this case.

In a truly self-similar evolution, we also expect velocities of particles to be a function of $[x/x_{nl}(a)]$. To test this we studied the behavior of the ratio $v_{3d}(a, x)/[\dot{a}x_{nonlinear}(a)]$ of the 3-dimensional velocity dispersion to our unit of velocity. Figures (2a,b,c,d,e,f) show the results for the different cases. It is seen that self-similarity (and the deviations from it) has the same pattern for velocity dispersion as for correlation functions: Figures (2a,b)

16

show time invariant behavior but (2c,d,e,f) do not. Note that Figure 2f shows the non-self-similar behavior of the open $n = -1$ model that is hidden in Figure 1f. Note also the somewhat surprising result that in all cases presented, the velocity difference between two particles is a rather weak function of their separation within $10^{\pm 1.5}$ of the nonlinear scale, especially for the self-similar cases.

4.2 Relative pair velocity, 'universality' and stable clustering

According to the arguments presented in section 2, we expect curve $h(\bar{\xi})$ to vary slightly but systematically as more small scale power is added. We indeed find such a behavior.

Figures (3a,b) show the behavior of h for $n = -2$ and $n = -1$ at three different redshifts $z = 1, 0.5, 0$. In the nonlinear end, the curves for $n = -1$ is lower than those for $n = -2$. That is, as we add more small scale power, the relative pair velocity decreases at nonlinear scales. This behavior is further borne out in the case of CDM (see Figure 3c) and HDM (see Figure 3d). In the redshift range considered, CDM model has an effective index which is between n=-1 and n=-2 and HDM has less small scale power than $n = -2$. The curve for CDM falls in between those for $n = -1$ and $n = -2$ and that of HDM is above the one for $n = -2$.

The behavior of $h(\bar{\xi})$ for the HDM model allows a simple test of the reasoning presented in section 2. To do this properly let us consider the evolution of a spherical top hat model in a background universe with some Ω along the lines of Gunn and Gott (1972). When $\Omega \neq 1$, we have $a(t) \propto (1 - \Omega^{-1})$ where Ω now refers to the instantaneous value at time t.

17

The quantity h can be estimated in the STH model by the relation $(1 + h) = (\dot{R}/R)(a/\dot{a})$, where $R(t)$ is the radius of the spherical region; similarly we may approximate $\bar{\xi}$ by the density contrast δ. Both these approximations are valid for $\bar{\xi} \gtrsim 1$ and should be interpreted as some average value. From the STH model it is easy to show that (with $\bar{\xi} \equiv \delta$),

$$1 + \bar{\xi} = \frac{(\mu - \sin \mu)^2}{(1 - \cos \mu)^3} \quad \frac{8 (\Omega - 1)^3}{\Omega^3 \left[\cos^{-1} \left(\frac{2}{\Omega} - 1 \right) - \frac{2}{\Omega} \sqrt{\Omega - 1} \right]^2}, \tag{16}$$

and

$$1 + h = \frac{(\mu - \sin \mu) \sin \mu}{(1 - \cos \mu)^2} \quad \frac{2 (\Omega - 1)^{3/2}}{\Omega \left[\cos^{-1} \left(\frac{2}{\Omega} - 1 \right) - \frac{2}{\Omega} \sqrt{\Omega - 1} \right]}, \tag{17}$$

where μ is the phase angle describing the evolution of the STH. It follows that

$$\frac{(1 + h)^2}{1 + \bar{\xi}} = \frac{\Omega}{2} \quad \frac{\sin^2 \mu}{(1 - \cos \mu)}. \tag{18}$$

This is valid for all values of Ω; equations (16) and (17) can be analytically continued for $\Omega \leq 1$. A nonlinear structure which is undergoing free-fall collapse, we will have $\mu \approx 2\pi - \epsilon$ with small ϵ and $\bar{\xi} \gg 1, h^2 \gg 1$. In this limit equation (18) becomes

$$h \cong \Omega_{eff}^{1/2} \bar{\xi}^{1/2}. \tag{19}$$

The subscript "eff" is a reminder that we should use an effective Ω which exists around most collapsing structures at the epoch of interest. [We are assuming that the shperical top hat region can be modelled as being located inside a larger region, which - when smoothed over the relevant scale - behaves like a universe with an effective Ω_{eff}.] Though it is difficult to model this quantity, two features are apparent: (1) At a given epoch,

18

$h \propto \bar{\xi}^{1/2}$ in the nonlinear phase. (2) As clustering produces underdense regions more and more collapsing structures will find themselves in $\Omega_{eff} < 1$ regions. As time goes on Ω_{eff} should decrease, and h should decrease at a given $\bar{\xi}$.

Figure 3d shows that both these expectations are borne out. The dashed lines at the nonlinear end has the slope of 0.5 which fits quite well to the simulation results. At a given $\bar{\xi}$, the h decreases as time goes on; at $z \approx 0$, we find $\Omega_{eff}^{1/2} \approx 0.3$.

In the case of Figures (3a,b) the key point to note is the lack of stable clustering. In both the cases, h does *not* approach unity asymptotically. This fact is more easily discernible using h than from mean correlation function. The value of h at a given $\bar{\xi}$ decreases as we add more small scale power, as expected. Note that lack of stable clustering invalidates the argument based on (12). Also note that these results disagree with the results of simulations discussed in Mo et al. (1995). They claim $\xi(a, x) \propto [\xi_L(a, l)]^{3/2}$ asymptotically, which requires $h = 1$ for large ξ. Our simulations show that $h \neq 1$ asymptotically.

The models described above all have $\Omega = 1$. To check the dependence on the background scale, we considered the behavior of $h[\xi]$ in the following cases: (i) a flat CDM + Λ model with $\Omega_{CDM} = 0.4$ and $\Omega_\Lambda = 0.6$ (model e) and (ii) an open model with $\Omega = 0.1$ and $P_k = Ak^{-1}$ (model f). These models have specific background scales and we find that it is reflected in $h[\xi]$ [see Figures (3e,f)]. The deviation in the linear end is

19

understandable since

$$h\left(a, x\right) \equiv -\frac{v_{\text{pair}}}{\dot{a}x} = \frac{2}{3}\left(\frac{a\dot{b}}{\dot{a}b}\right)\bar{\xi}\left(a, x\right).$$ (20)

where $b\left(t\right)$ is the growing solution to the linear perturbation equation. For reasonable Ω, we can approximate $(a\dot{b}/\dot{a}b)$ by $[\Omega\left(z\right)]^{0.6}$. This formula is used usually at $z = 0$; it is a reasonable approximation at moderate z, if the instantaneous value of Ω is used. So, in the linear end $h \propto [\Omega\left(z\right)]^{0.6}$ at a given $\bar{\xi}$ and this is indeed seen in figure 3 (e, f). At the nonlinear end, h seems to approach unity within the limits of our resolution. This suggests that models with $\Omega < 1$ obey the hypothesis of stable clustering to a better approximation than models with $\Omega = 1$. This is understandable since structures freeze out in the $\Omega < 1$ model around $z \approx \Omega^{-1} - 2$; in contrast, significant merging takes place in $\Omega = 1$ universe at all epochs. In the intermediate scales, no clear pattern emerges in these models.

4.3 Relation between $\bar{\xi}$ and $\bar{\xi}_L$

The original ansatz can also be presented as a relationship between $\bar{\xi}(a, x)$ and $\bar{\xi}_L(a, l)$. In the case of strict universality, these two approaches are related by equation (9). However, when deviations from universality are present, it is worthwhile to examine both independently. Figures (4a,b,c,d,e,f) show the results for different cases. These figures relate the nonlinear correlation function at a scale x to linear correlation function at a scale l where $l = x(1 + \bar{\xi})^{1/3}$. The relation between l and x is independent of the value of Ω and can be derived by the method of characteristics used by NP. The broken lines in these figures have slopes 1 and 1.5 as suggested by equation (10). We find that

20

the deviations from our ansatz, seen in h, give rise to corresponding deviations in these figures. A spectral dependence is evident in Figures 4a and 4b, as well as in the slight shift for the CDM case, Figure 4c .This dependence seems to be in the same sense as reported by Mo et al, 1995. The deviations from stable clustering follows the pattern discussed earlier, except for Figure 4f. When $\Omega \neq 1$, we have $\xi_L = b^2(t)x^{-(n+3)}$ and $\xi = a^3 F(ax)$; in that case, stable clustering assumption does not translate into a simple scaling of the form $\xi \propto \xi_L^{3/2}$. By and large, these figures reinforce the conclusions arrived at earlier.

4.4 Overall Conclusions

1) As expected, (but contrary to some earlier work), we find that if the input P_k has a power law dependence on k, then the only scale that is relevant is the scale at which mass fluctuations are nonlinear, x_{NL}, which induces a break in the input (linear) power spectrum. Under these circumstances all quantities that we have measured show a self-similar evolution, i.e., they are only functions of scaled radius x/x_{NL}.

2) The "stable clustering" assumption is not true in general, presumably because, in the case of $\Omega = 1$, there is steady merging of structures so that isolated bound objects do not survive intact, violating the key ansatz behind the stable clustering hypothesis. When $\Omega < 1$, since structure freezes out at low redshift, the stable clustering model is a better approximation than if $\Omega = 1$.

3) The relation between the dimensionless pair velocity $h(a,x) = -v_{pair}/Hr$ and the mean correlation function $\bar{\xi}(a,x)$ is not universal because of the failure of the stable

clustering assumption although within the range of cosmologically plausible models the relation $h(\bar{\xi})$ shows sufficiently uniform behavior to be a useful quantity.

REFERENCES

Bardeen, J.M., Bond, J.R., Kaiser, M., and Szalay, A.S. 1986, ApJ, 304, 15

Brieu, P.P., Summers, F.J., & Ostriker, J.P. 1995, ApJ, submitted

Bagla, J.S. and Padmanabhan, T. 1993, IUCAA preprint 22/93; based on the lecture given at VI th IAU Asia-Pacific Regional Meeting on Astronomy, Aug,93; to appear in Jour. Astrophys. Astronomy.

Bagla, J.S. and Padmanabhan, T. 1995, Evolution of gravitational potential in the quasilinear and nonlinear regimes, IUCAA preprint 8/95;astro-ph 9503077.

Cen, R. 1992, ApJS, 78, 341

Cen, R., Gnedin, N.Y., & Ostriker, J.P. 1993, ApJ, 417, 387

Efstathiou, G., & Eastwood, J.W. 1981, MNRAS, 194, 503

Efstathiou, G., Davis, M., Frenk, C.S., & White, S.D.M. 1985, ApJS, 57, 241

Efstathiou, G., Frenk, C.S., White, S.D.M., & Davis, M. 1988, MNRAS, 235, 715

Hamilton A.J.S., Kumar, P., Lu E., & Mathews, A. 1991, ApJ, 374, L1

Hockney, R.W., & Eastwood, J.W. 1981, "Computer Simulations Using Particles", McGraw-Hill, New York.

Gunn, J.E., & Gott, J.R., III 1972, ApJ, 176, 1

Mo, H. J., Jain, B., & White, S. D. M. 1995, MNRAS, submitted

Nityananda, R., & Padmanabhan, T. 1994, MNRAS, 271, 976

23

Okumura, S. K., et al. 1993, PASJ, 45, 329

Park, C.B. 1990, MNRAS, 242, 59

Peebles, P.J.E. 1980, "The Large-Scale Structure of the Universe" (Princeton: Princeton University Press)

FIGURE CAPTIONS

Fig. 1– Figures (1a,b,c,d,e,f) show the two-point correlation function as function of r/r_{nl} (where r_{nl} is the scale corresponding to $\xi = 1$) at three different redshifts [$z = 0, 0.5, 1$ with (solid, dotted, dashed) curves, respectively; this order will be maintained in subsequent figures] for Models (a,b,c,d,e,f) listed in Table 1. Also shown as two dashed lines in each figure are asymptotic slopes at the extreme nonlinear and linear ends. Note that figure 1 (a,b), which are for powerlaw spectra in $\Omega = 1$ universe, show the expected self similar behaviour while the other figures do not.

Fig. 2– Figures (2a,b,c,d,e,f) show the ratio $v_{3d}(a, x)/[\dot{a}x_{nonlinear}(a)]$ between the 3-dimensional pairwise velocity dispersion to our velocity unit, as a function of r/r_{nl} at three different redshifts ($z = 0, 0.5, 1$) for Models (a,b,c,d,e,f). Figure 2 (a,b), which are for powerlaw spectra in $\Omega = 1$ universe, show the expected self similar behaviour while the other figures do not.

Fig. 3– Figures (3a,b,c,d,e,f) shows h as a function of $\bar{\xi}$ at three different redshifts [$z = 0, 0.5, 1$ with (solid dots, open circles, open squares), respectively; this order will be maintained in subsequent figures] for Models (a,b,c,d,e,f). The errorbars are shown for 1σ statistical

uncertainties. In the nonlinear end the h is lower for a given $\bar{\xi}$ if there is more small scale power. The value of h in the asymptotic limit depends on the spectrum and does not always go to unity; this shows that stable clustering is not a valid assumption in general.

Fig. 4– Figures (4a,b,c,d,e,f) show $\bar{\xi}$ as a function of $\bar{\xi}_L$ at three different redshifts $(z = 0, 0.5, 1)$ for Models (a,b,c,d,e,f).

Table 1. Summary of the computed models

Run	Model	Code	Ω	Λ	$L_{box}h^{-1}Mpc$	$l_{res}h^{-1}Mpc$	σ_8
a	$P_k = Ak^{-2}$	PM	1	0	128	0.18	1.05
b	$P_k = Ak^{-1}$	P^{3}M	1	0	128	0.025	1.05
c	SCDM	P^{3}M	1	0	128	0.025	1.05
d	HDM	PM	1	0	128	0.18	1.05
e	LCDM	P^{3}M	0.4	0.6	128	0.025	0.79
f	Open $P_k = Ak^{-1}$	PM	0.1	0	128	0.18	1.05

Figure 1a
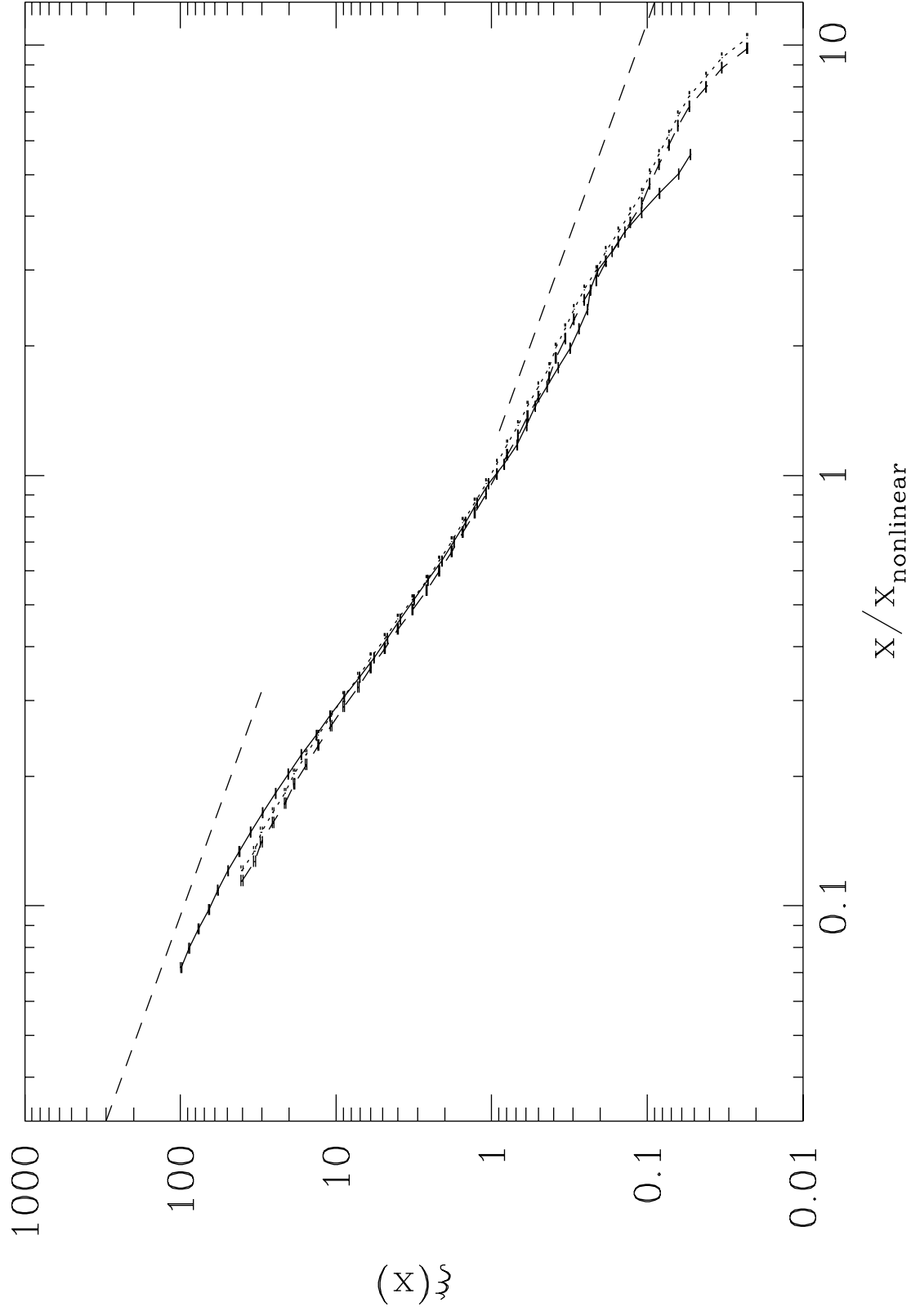
Figure 1b
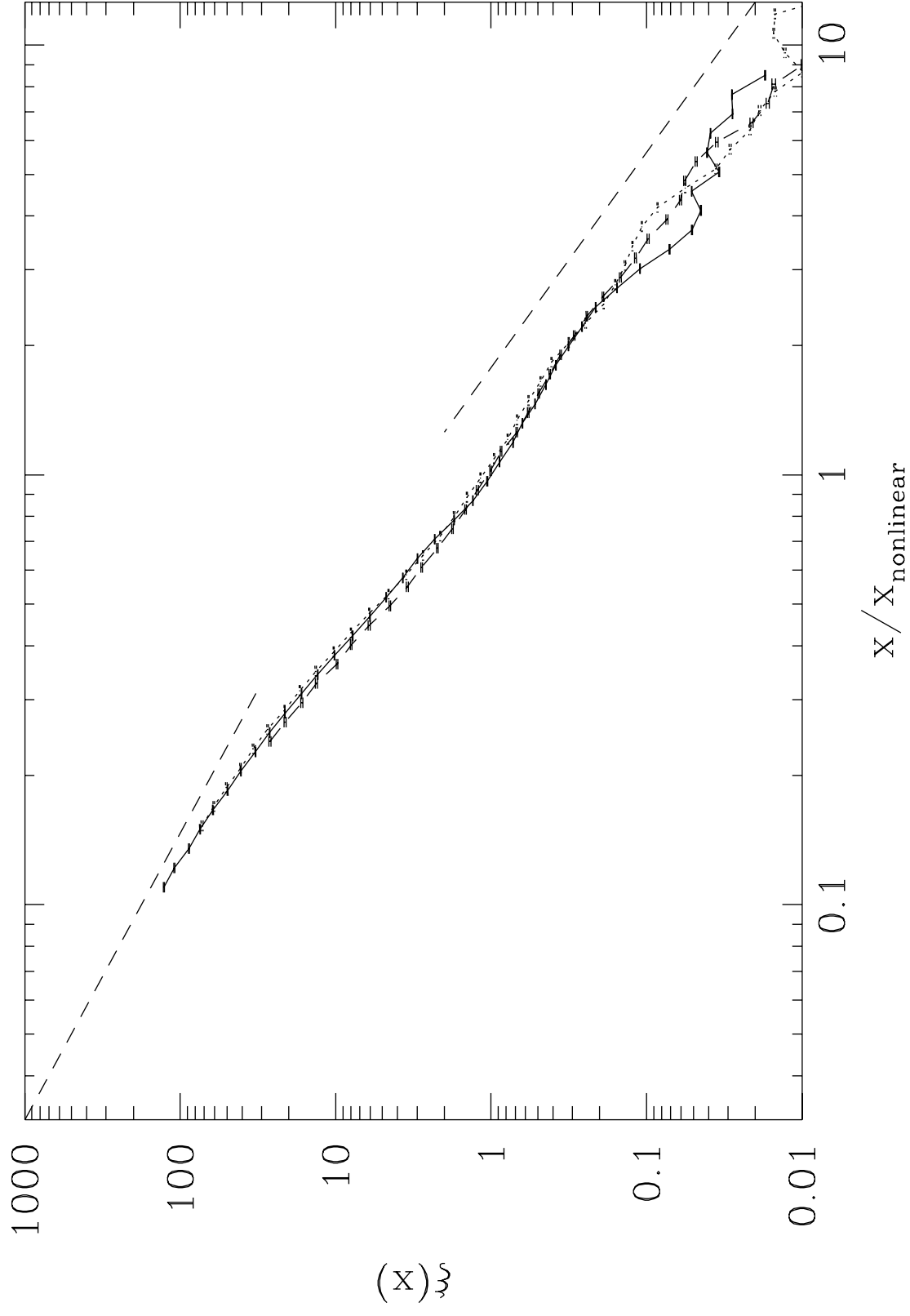
Figure 1c
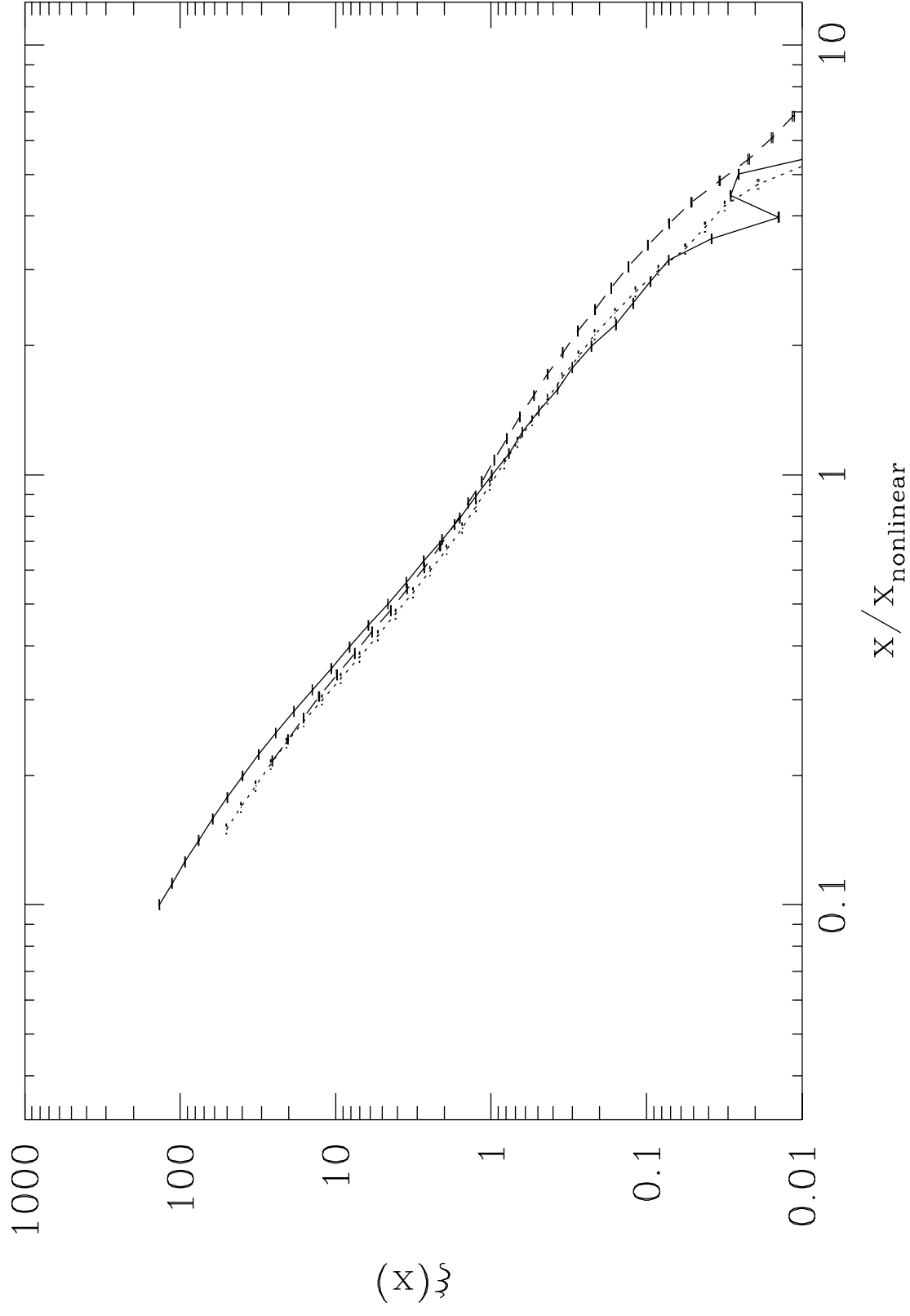
Figure 1d
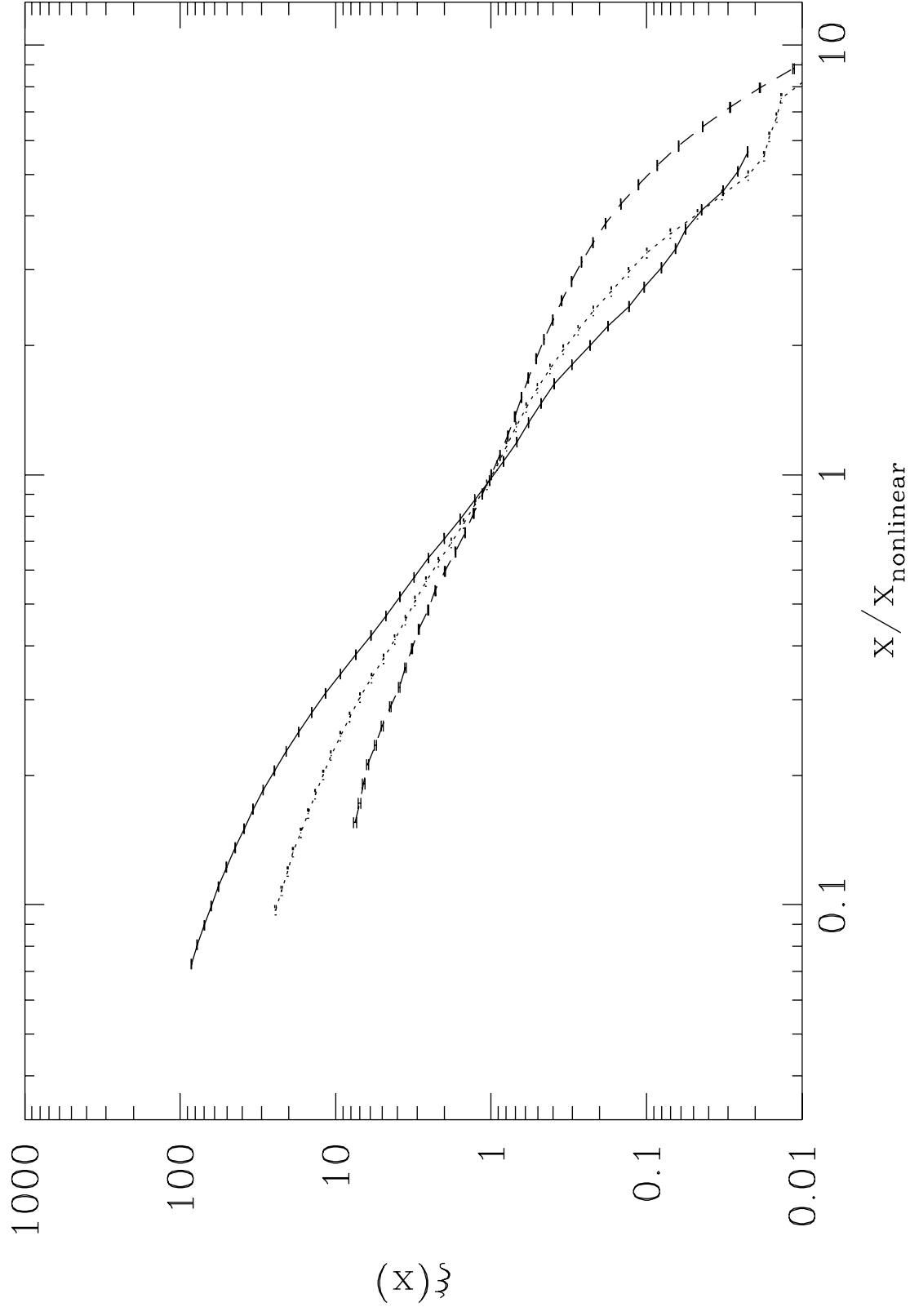
Figure 1e
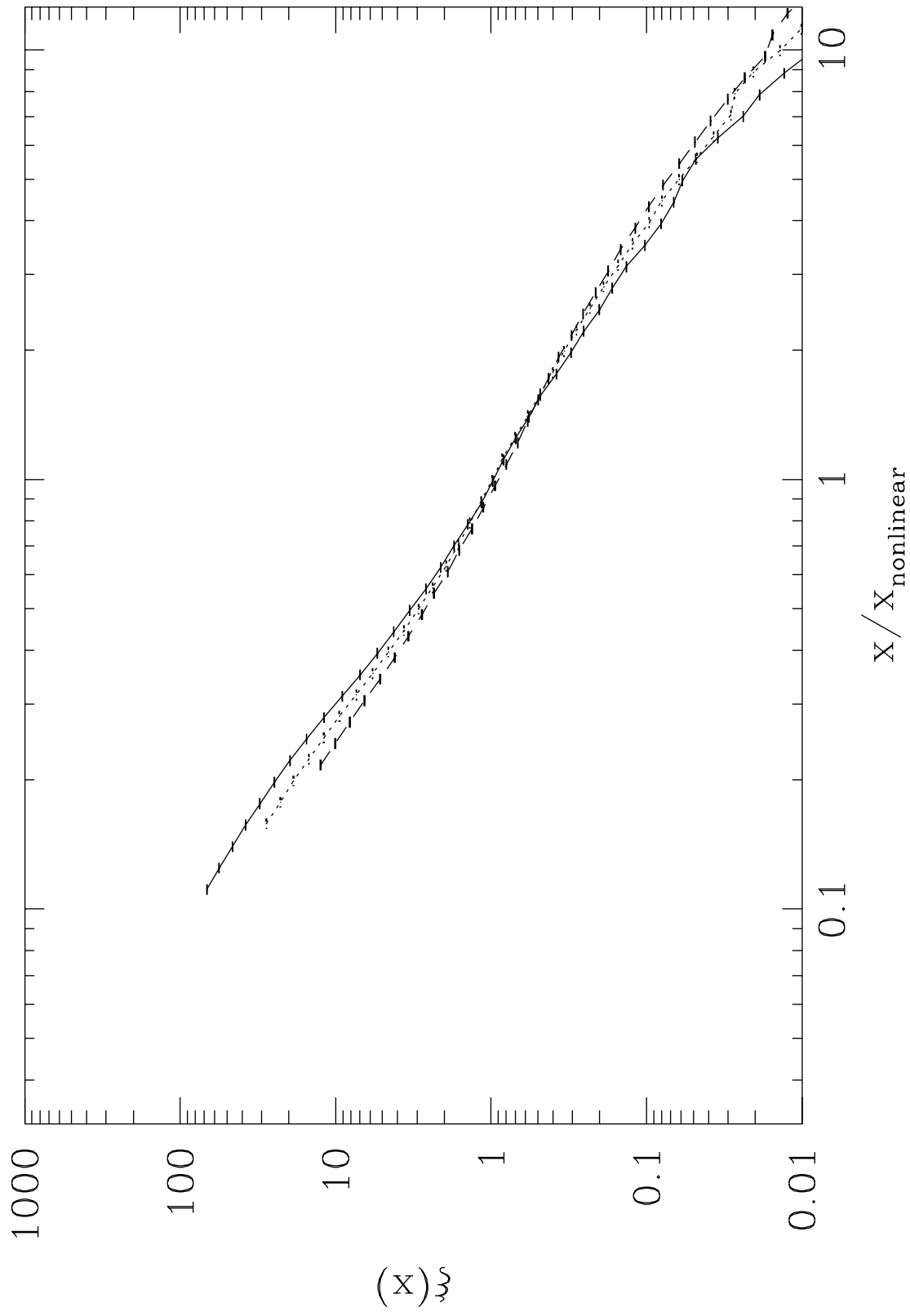
Figure 1f
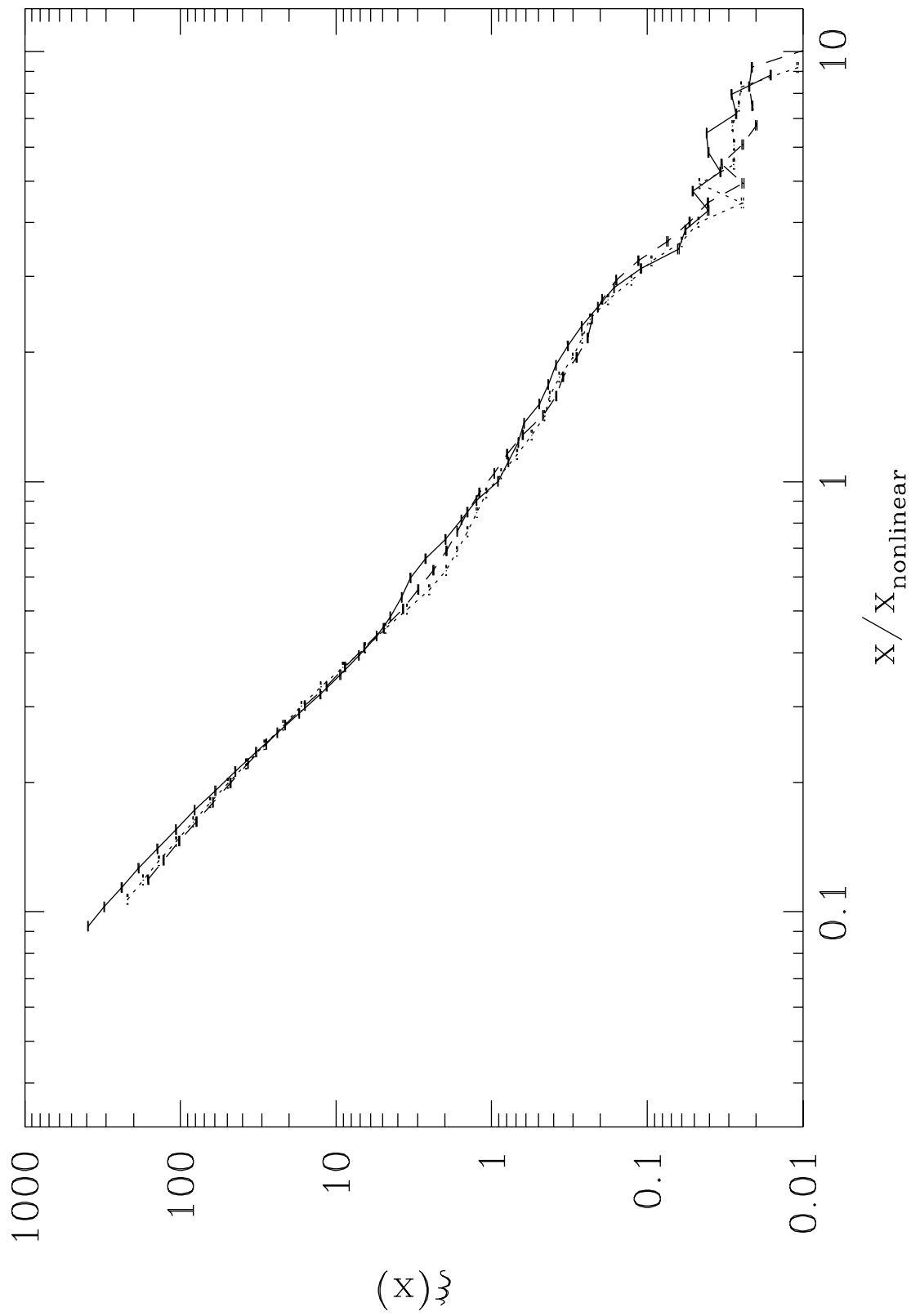
Figure 2a
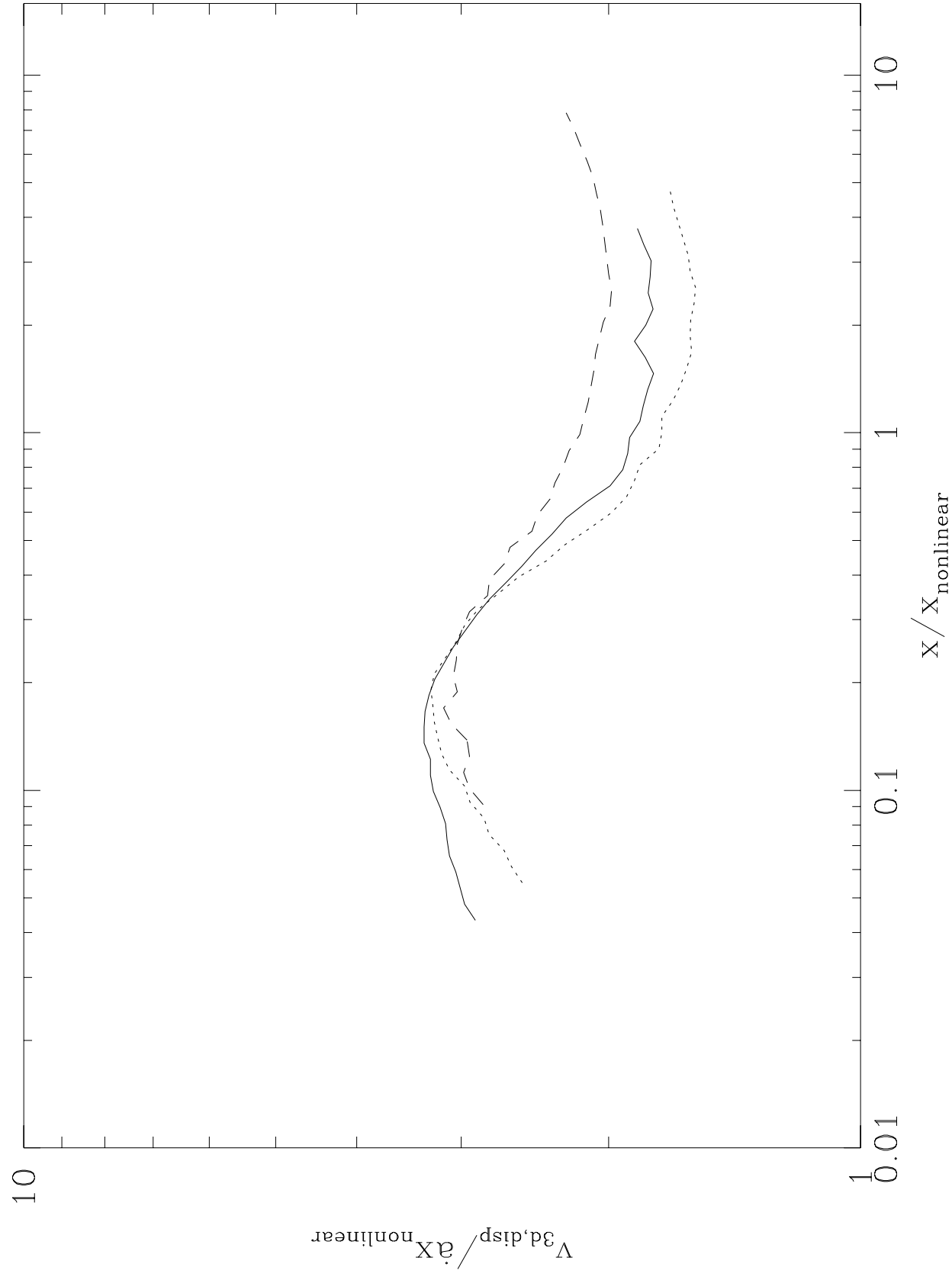
Figure 2b

Figure 2c

Figure 2d

$V_{3d,disp}/\dot{a}x_{nonlinear}$

$x/x_{nonlinear}$
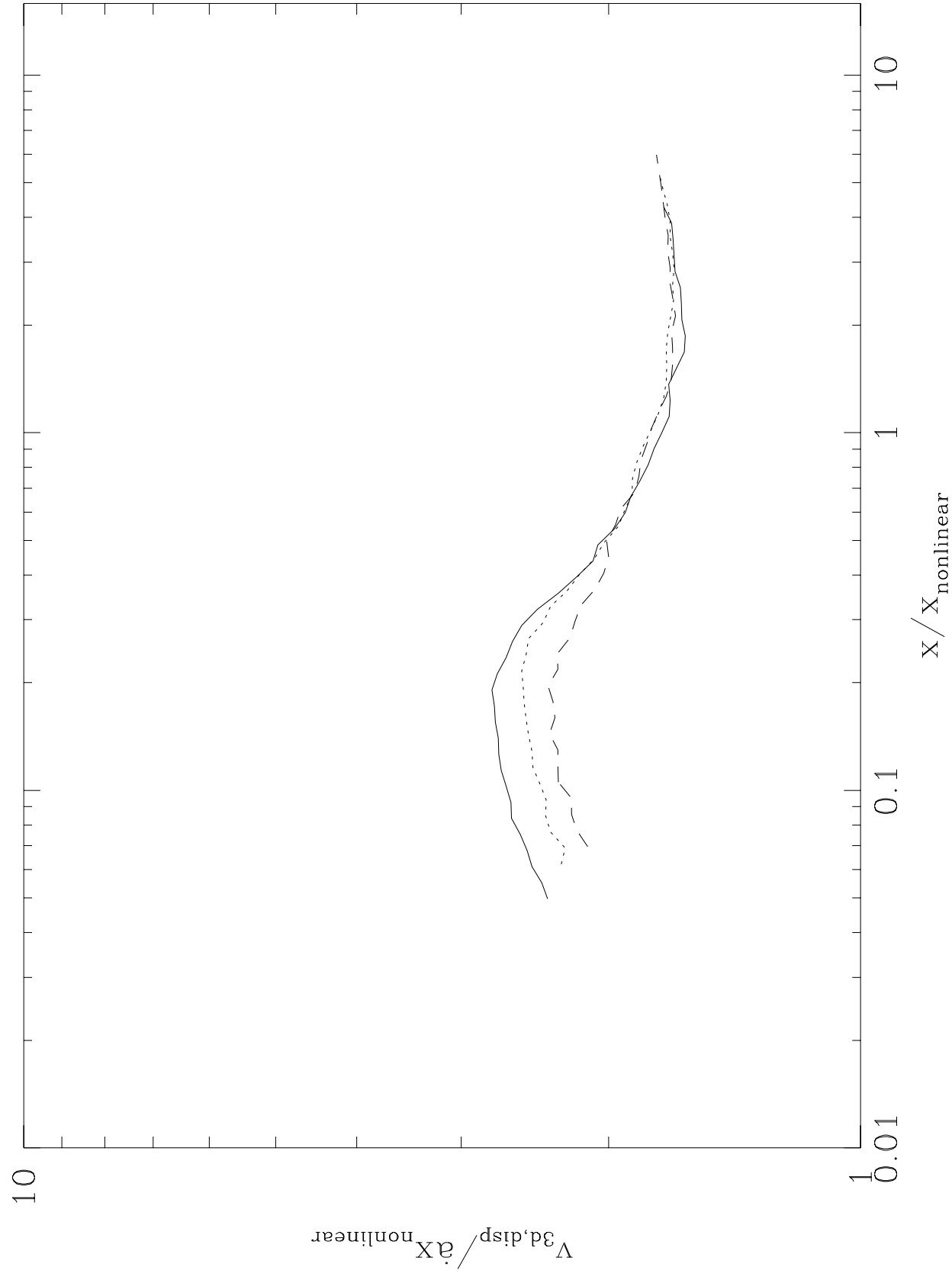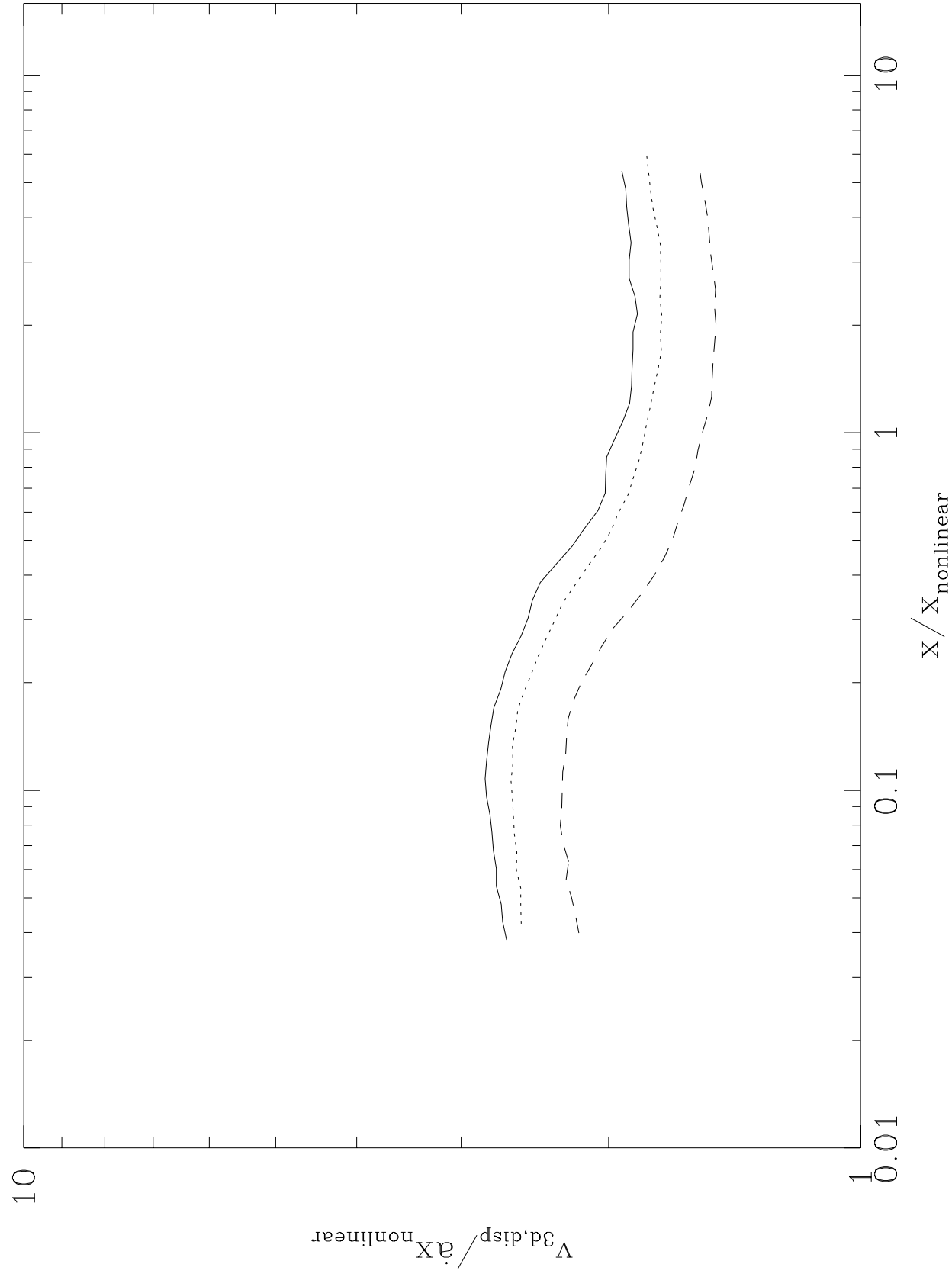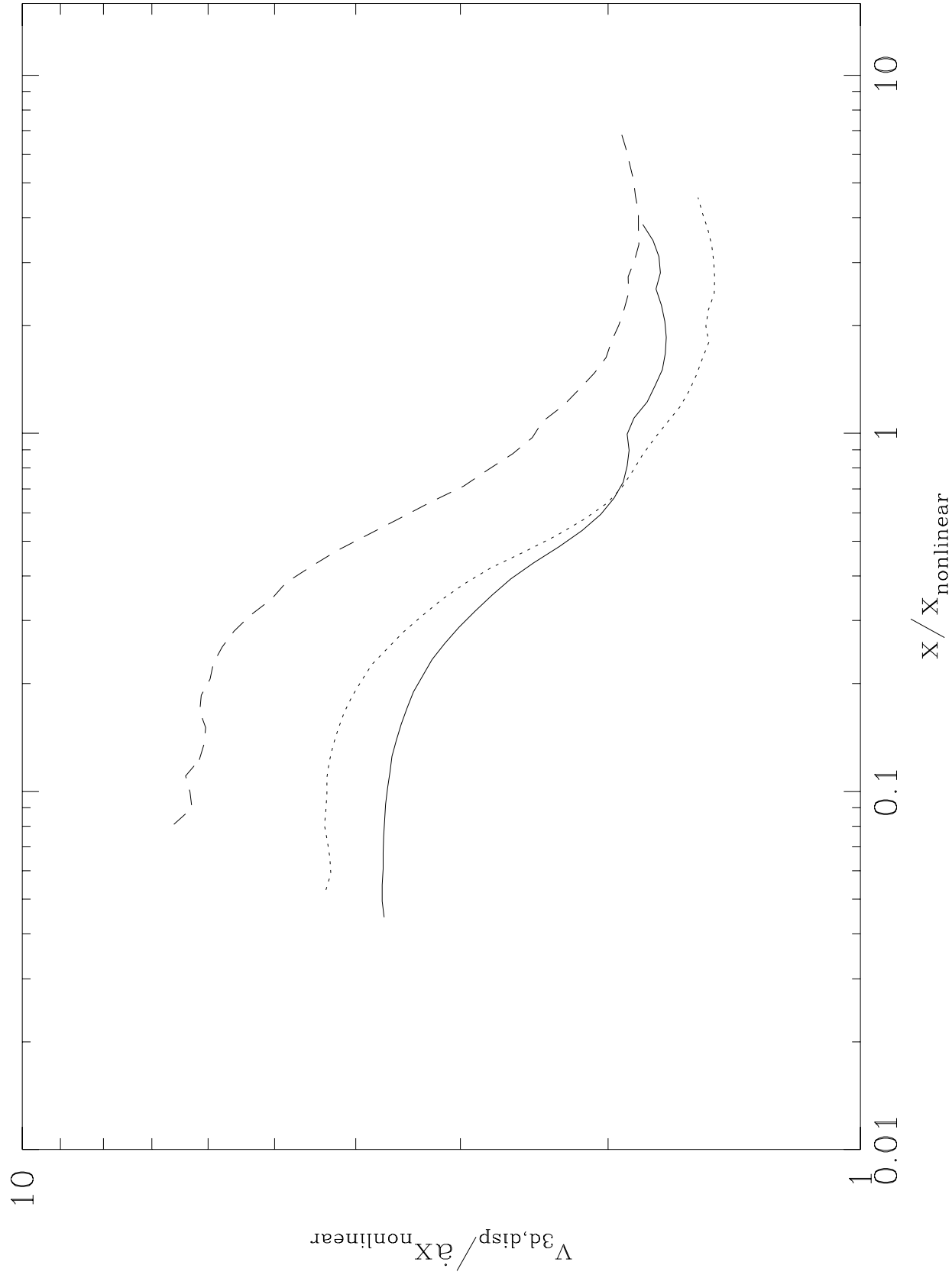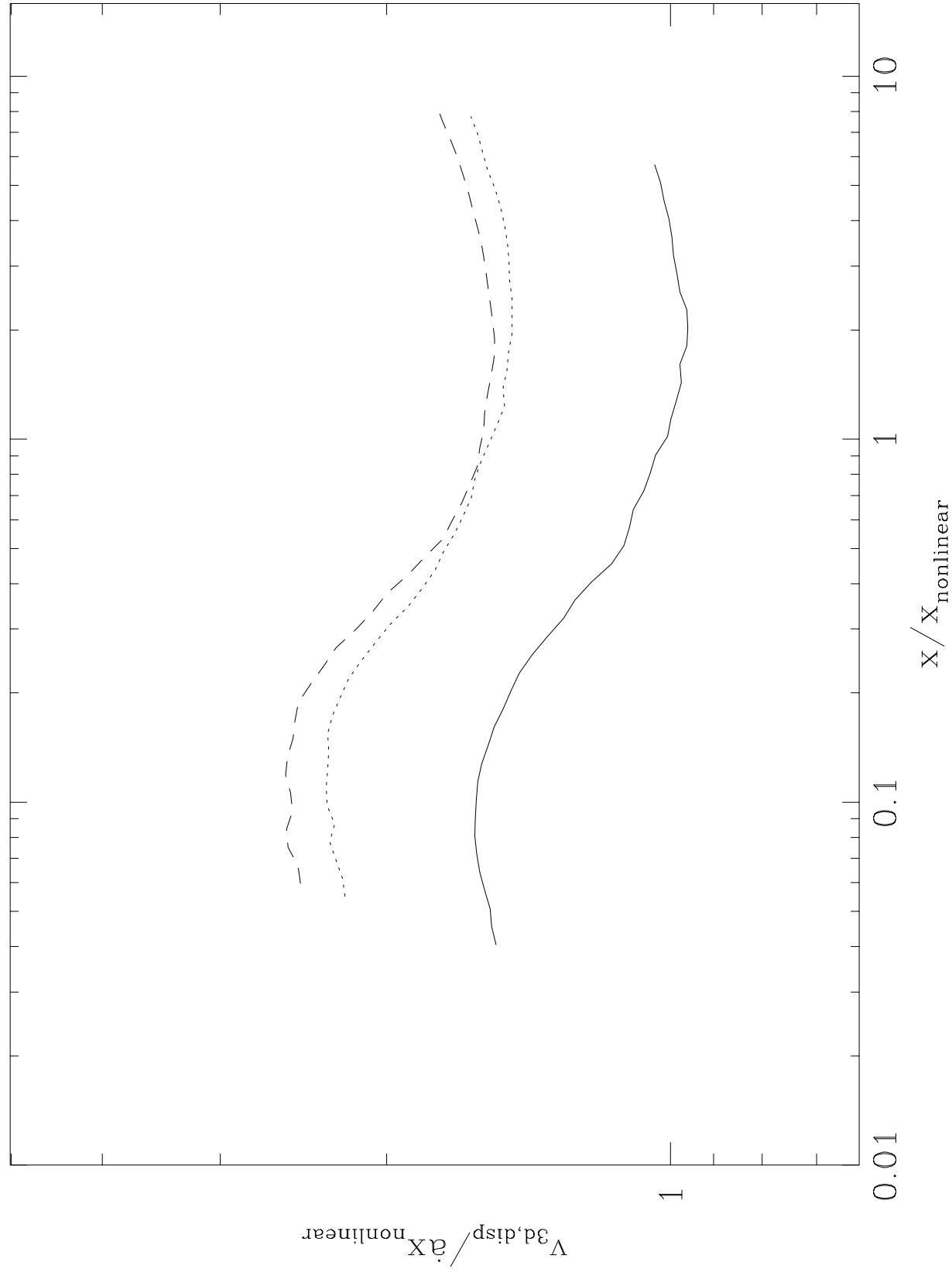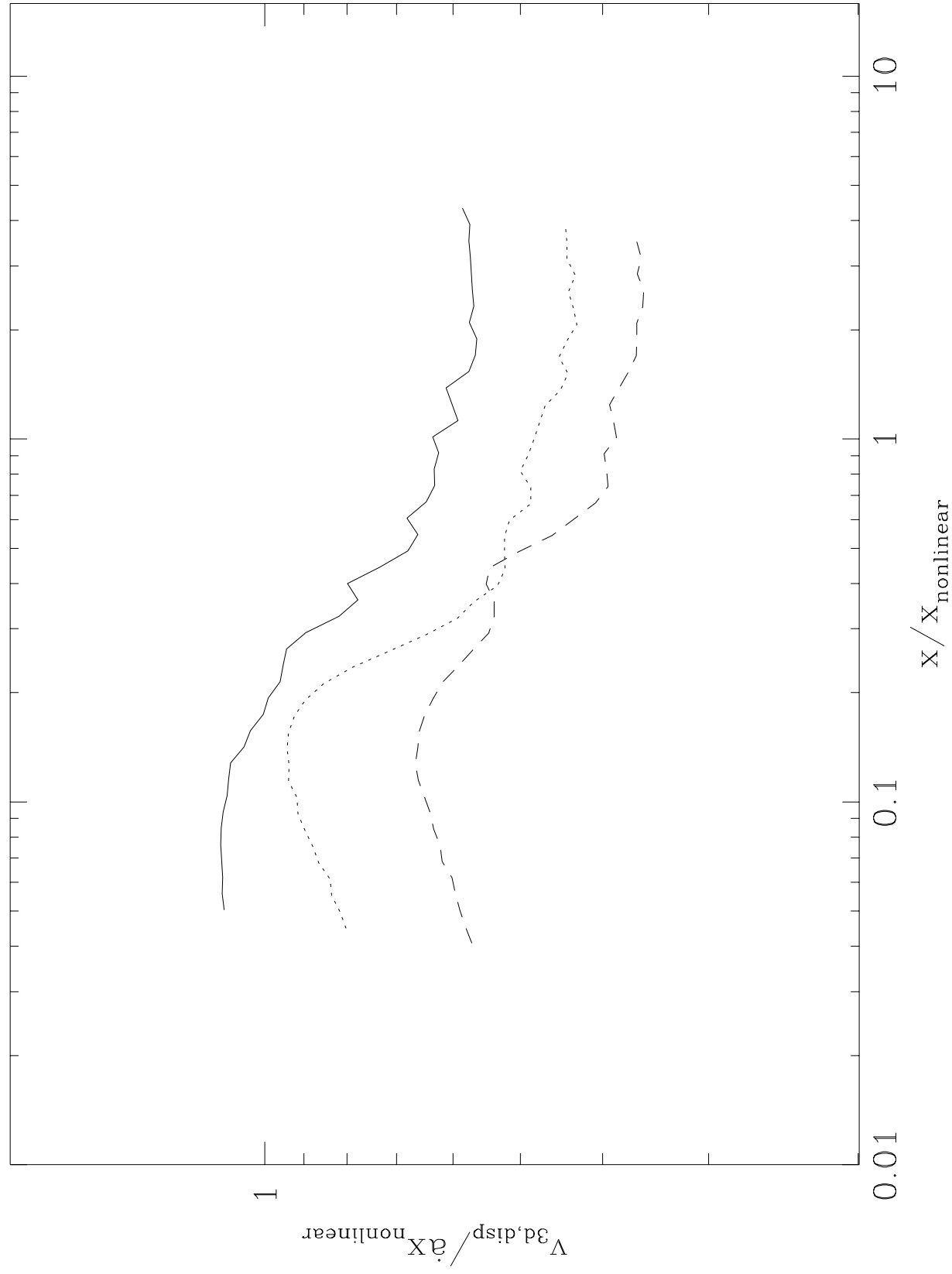
Figure 2e

Figure 2f

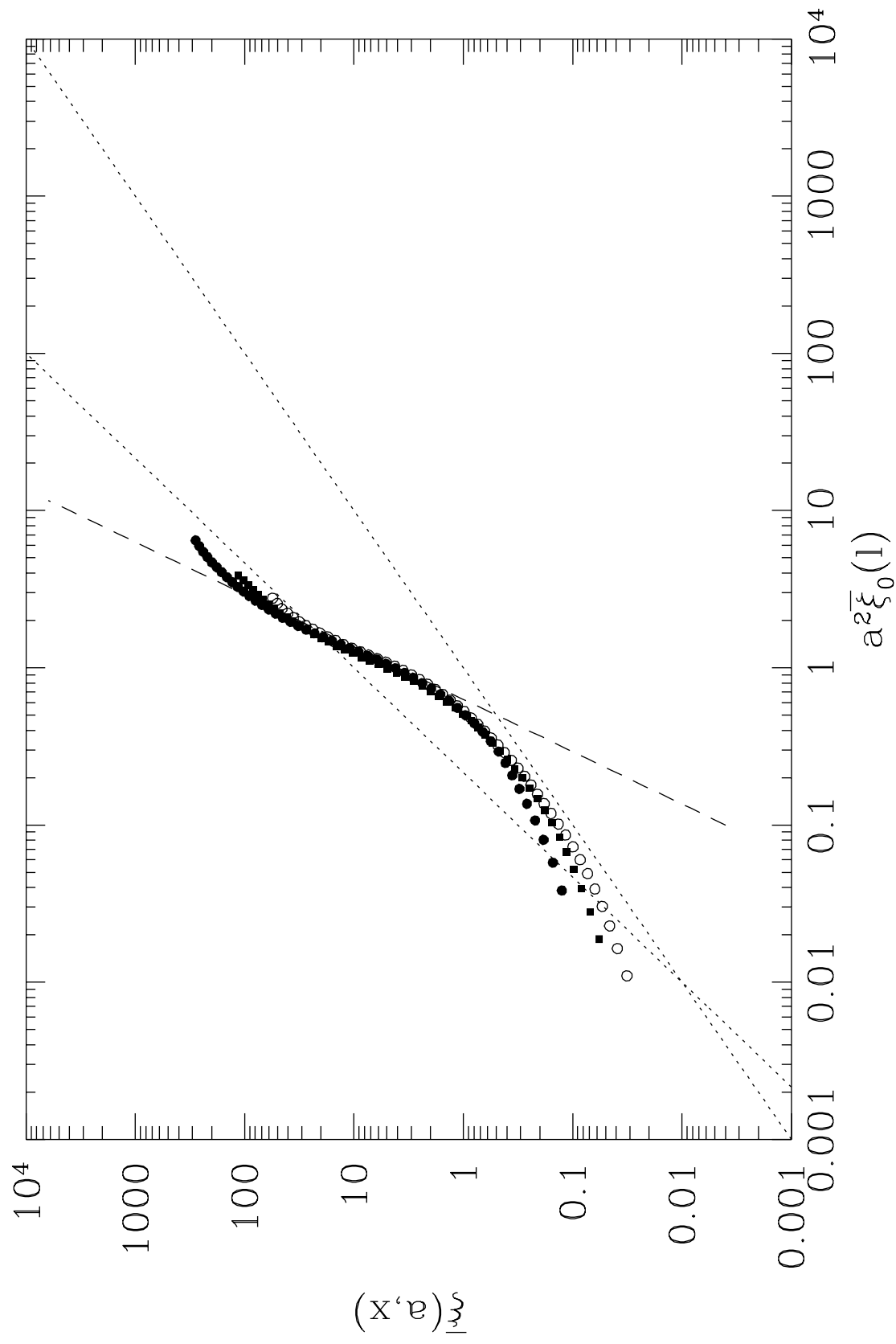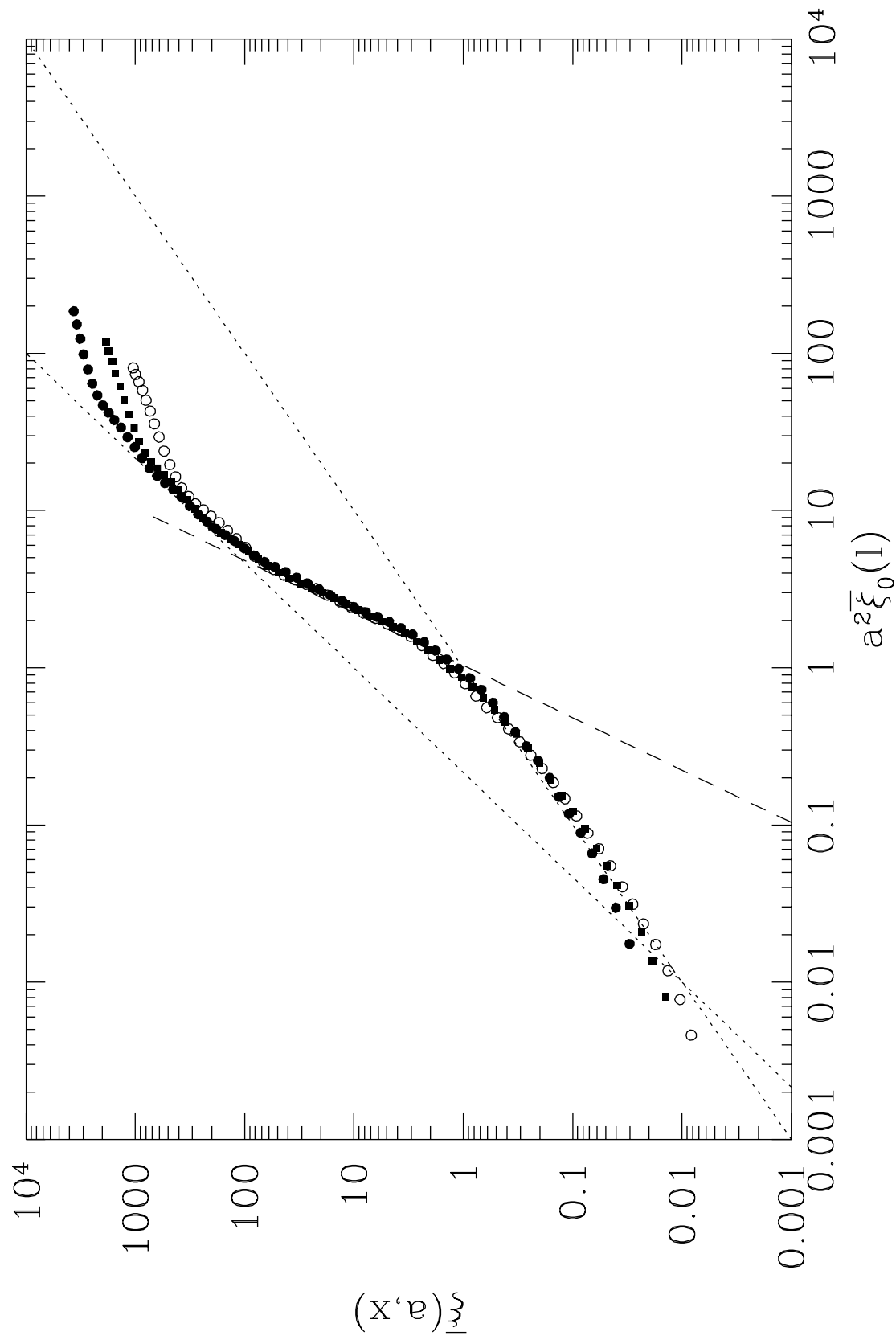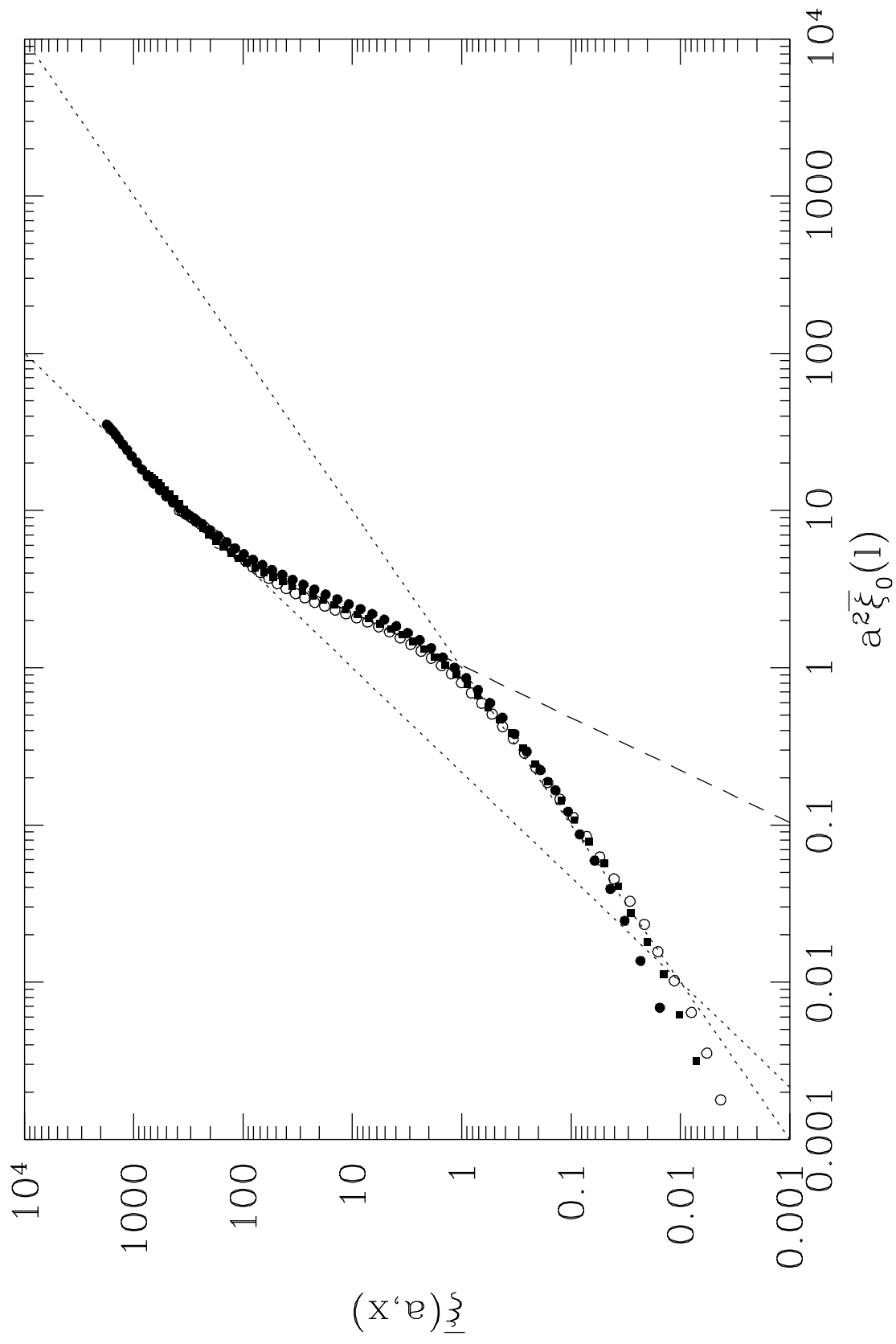Figure 3a
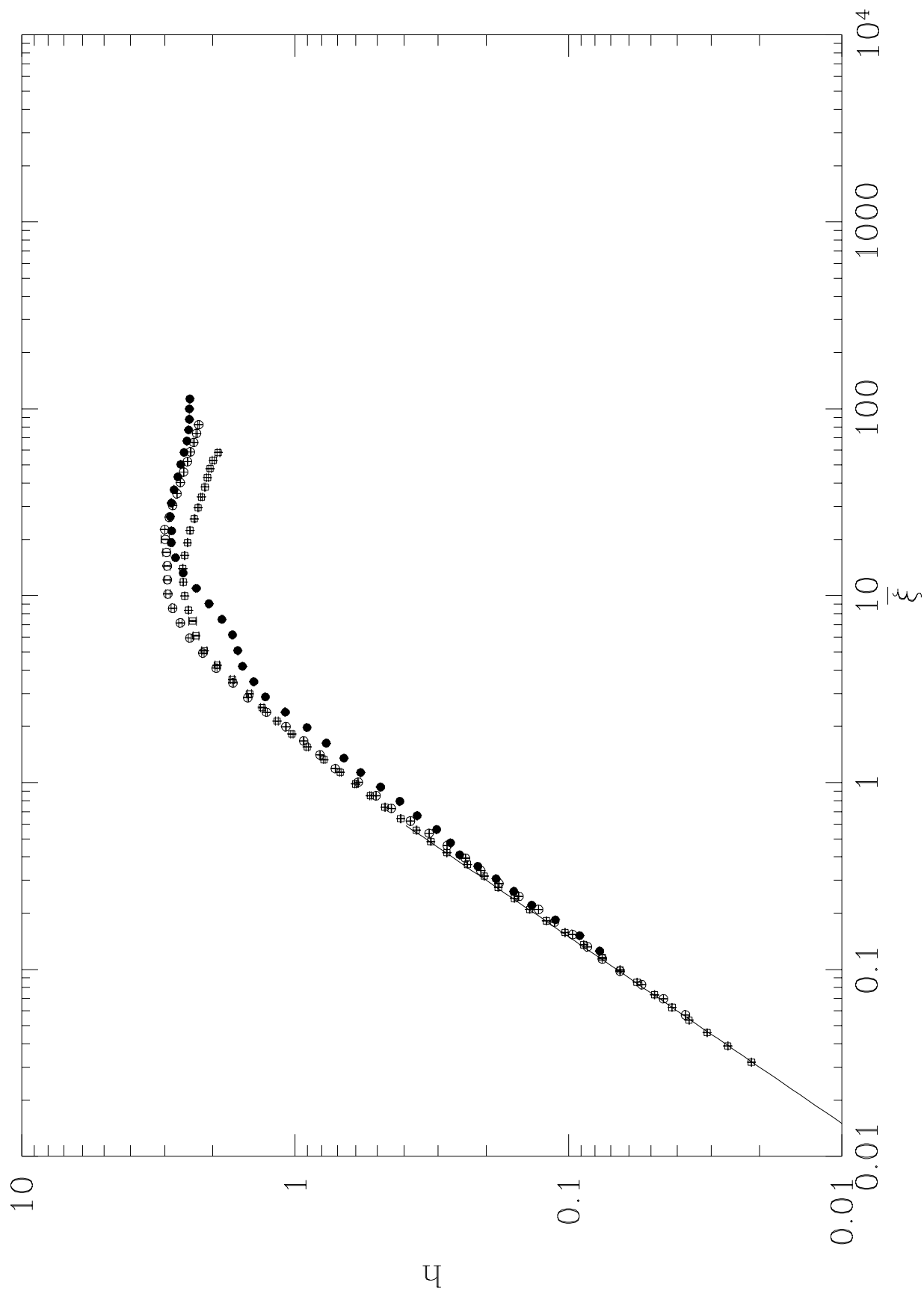
Figure 3b
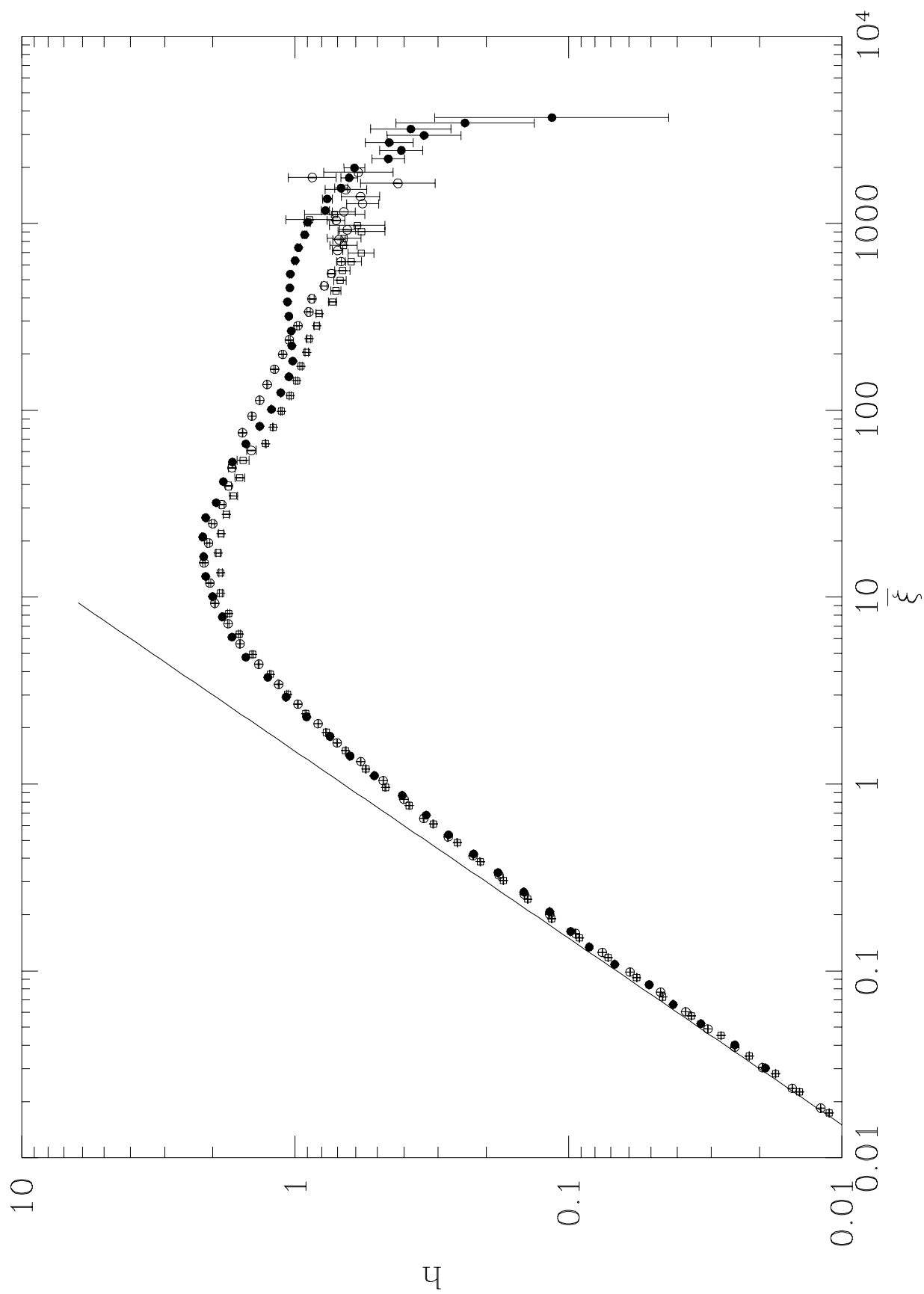
Figure 3c
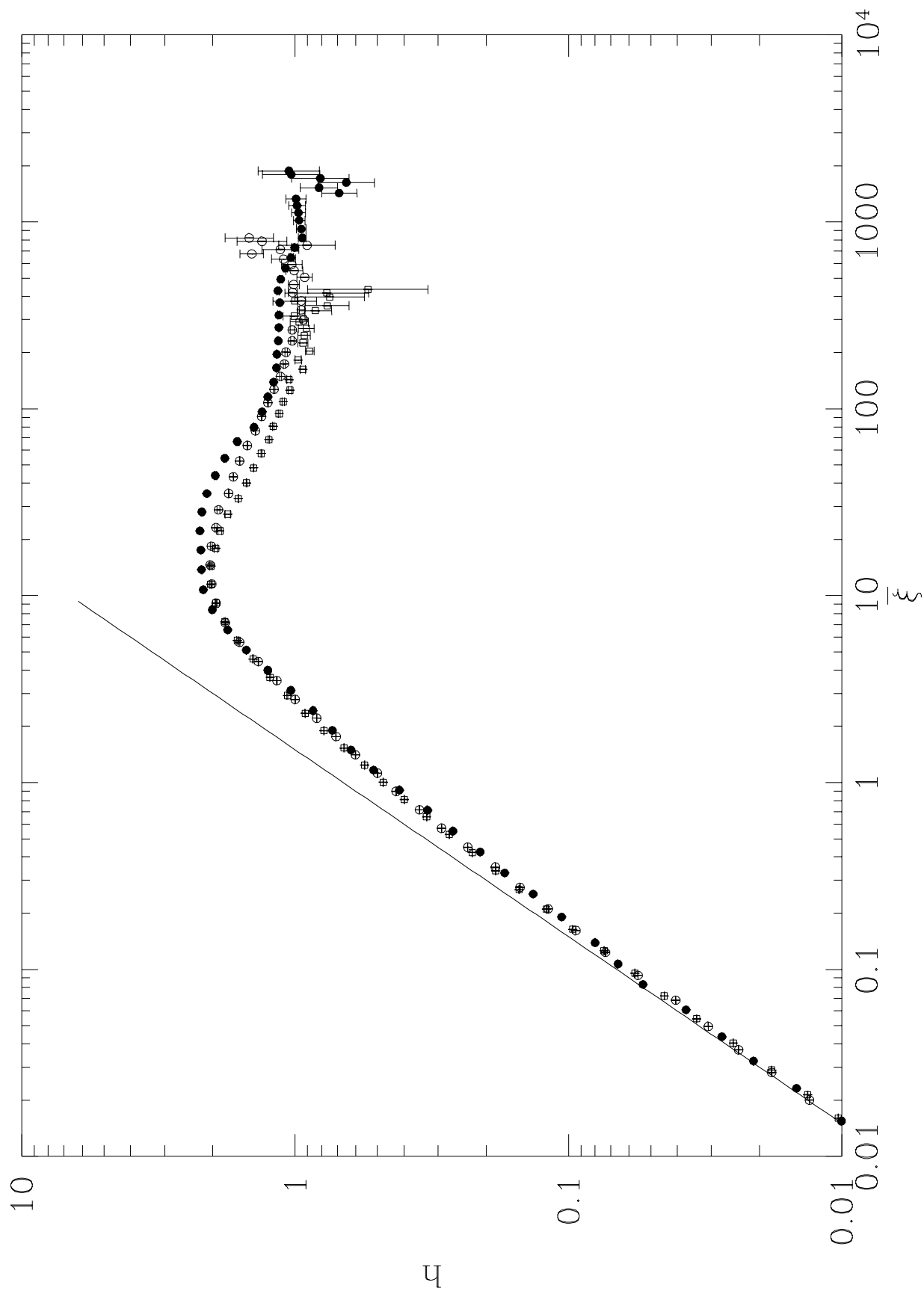
Figure 3d
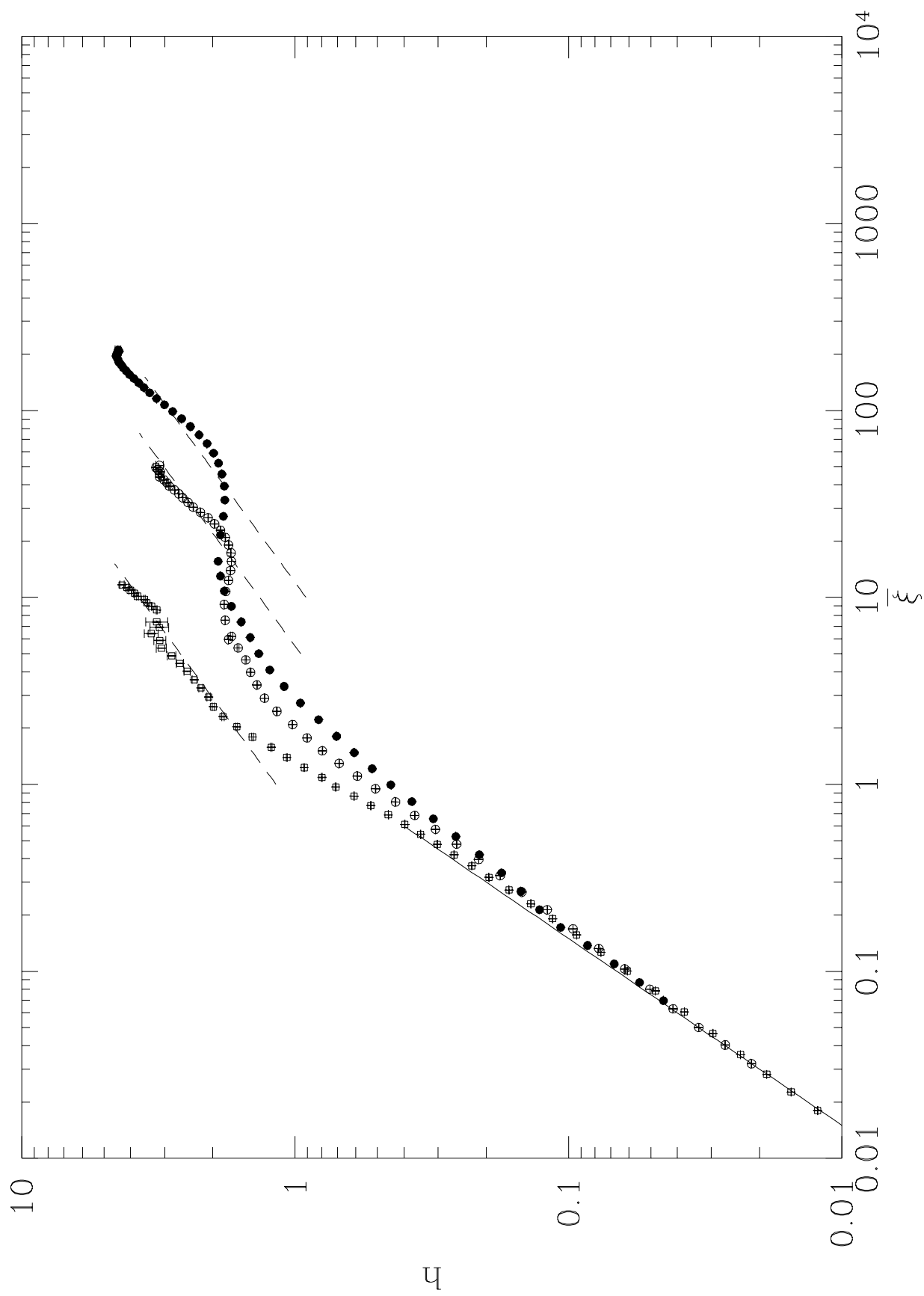
Figure 3e
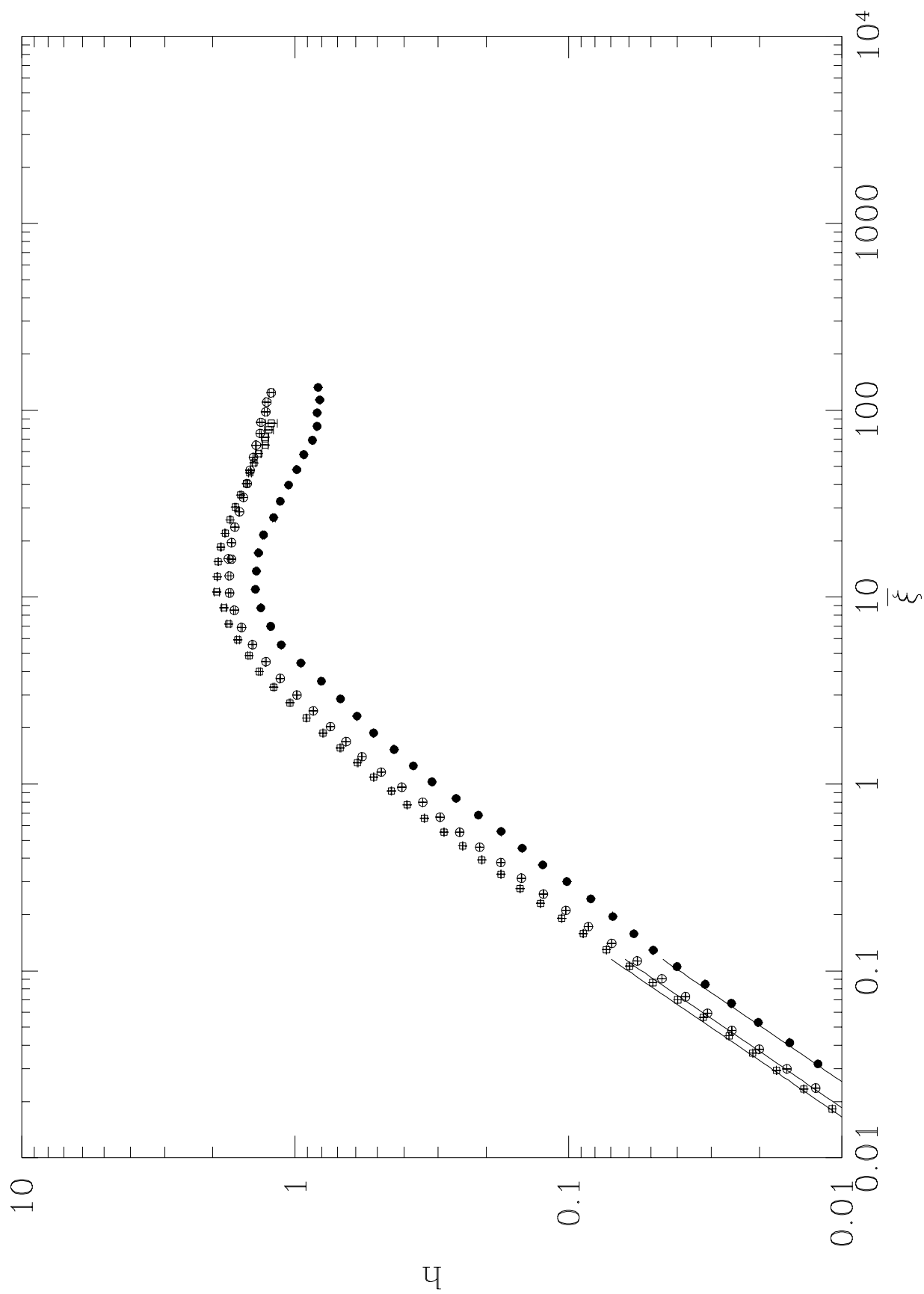
Figure 3f
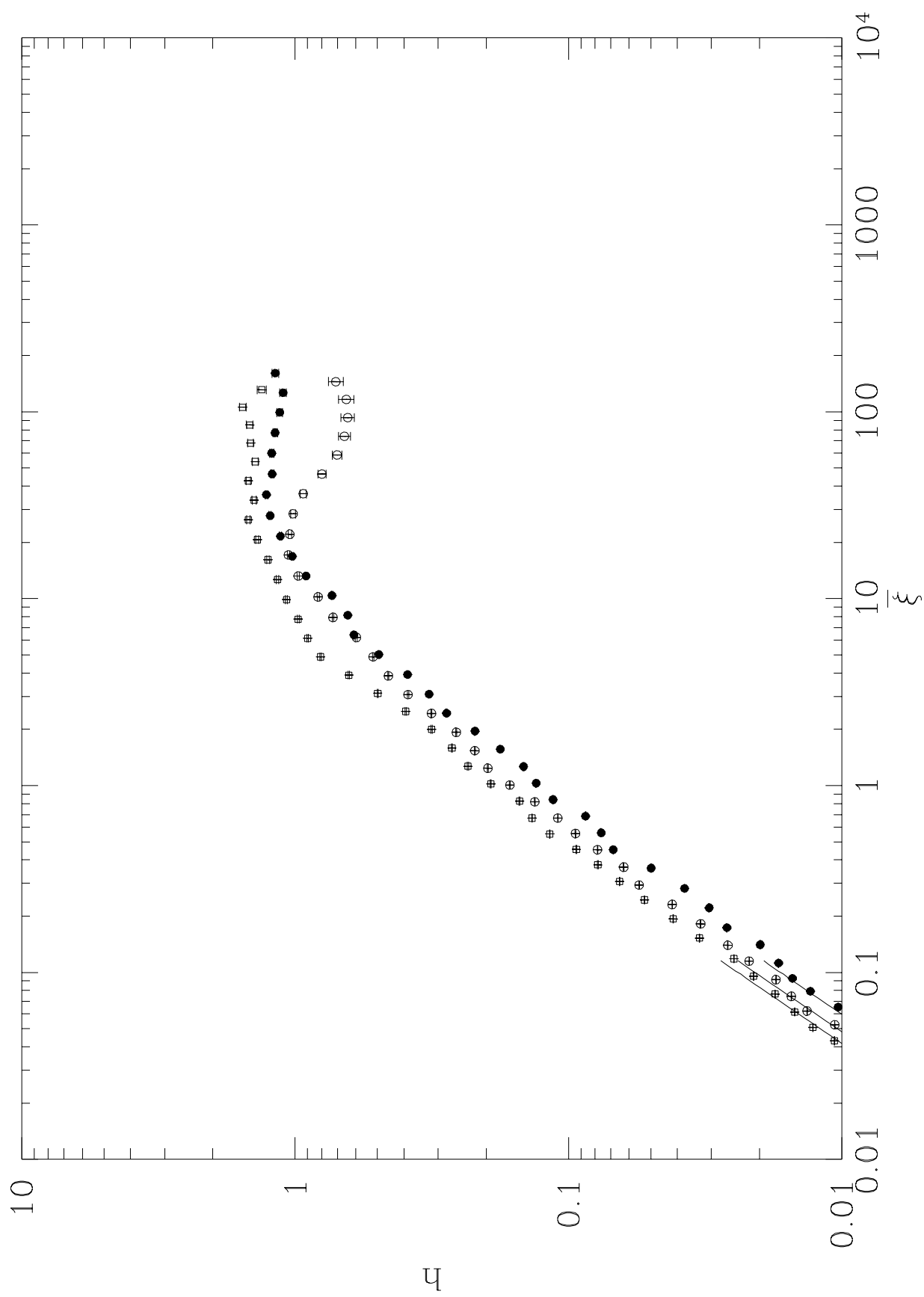
Figure 4a

Figure 4b

Figure 4c

Figure 4d

Figure 4e

$a^2 \bar{\xi}_0(l)$

$\bar{\xi}(a,x)$

Figure 4f